We wish to thank all three reviewers for their detailed comments and thoughtful suggestions.

1 Reply to the comments of reviewer 1

It appears that the comments from reviewer 1 refer to the first version submitted to ACPD and not to the version published online. As a result, the line numbers do not match the online version.

1. **There should be some discussion early on in the paper about the bidirectional flux of NH3. It is now only mentioned as future work, but the lack of consideration of this in the current modeling has implications that should be discussed.**

   We have added the following text to the method section:

   The bidirectional exchange of ammonia is not represented in AM3-LM3-DD [Massad et al., 2010, Flechard et al., 2013]. This reflects in part uncertainties in the emission potential of vegetation and the lack of detailed treatment of agricultural activities in LM3 [Riddick et al., 2016]. We thus expect AM3-LM3-DD to overestimate NH_3 *dry deposition in source regions [Zhu et al., 2015, Sutton et al., 2007].*

   As a result, we expect that the simulated enhancement of N deposition over natural tiles relative to the average deposition over all land tiles may be an underestimate. This has been clarified in the analysis of the results as follows:
   The enhancements of the dry deposition of NH_x *over natural vegetation is likely to be underestimated in AM3-LM3-DD as the surface bidirectional exchange of* NH_3 *tends to reduce its deposition in source regions.*

2. **Line 44: Characterizing dry deposition as just surface resistance is not really accurate.**
   This has been removed.

3. **Line 46: The Schwede and Lear (2014) reference is not the appropriate one for the wet deposition fluxes as the values used are those from the National Atmospheric Deposition Program National Trends Network.**
   This section had been removed in the online version of the manuscript.

4. **Line 55: The role of organic nitrogen should be discussed as well as other unmeasured components of the nitrogen budget that are currently only widely available from models.**

   We have added the following text in the discussion of the SOAS data:

   We find that ($\alpha = 7$, $\beta = 1$) *provide a reasonable fit for all organic nitrates. These parameters imply that the deposition of isoprene-derived organic nitrates is primarily controlled by dry cuticles with small contributions of stomata and stems. We note that these parameters imply a much greater solubility and reactivity of organic nitrogen than in other models (e.g.,* $\alpha = 0$, $\beta = 0.5$ *in AURAMS [Zhang et al., 2002]). While we use these parameters globally, such large differences warrant further investigations, as the deposition of organic nitrogen may account for over 25% of the overall N deposition but remains rarely measured [Jickells et al., 2013].*

5. **Lines 72-79: Greater emphasis could be provided here that a new model has been developed for including in AM3. It is not simply that you used an approach already in another model. You combined pieces from different models.**

   The text was revised as follows:
   Here, we describe the development of a new model, in which dry deposition of gaseous and aerosol species are calculated within the dynamic vegetation model LM3 [Shevliakova et al., 2009, Milly et al., 2014]. The combined model will be referred to as AM3-LM3-DD hereafter.

6. **Line 80-93: The tile structure is a bit confusing and it is not clear in the use of primary and secondary tiles and what information is contained at each level. What are the categories for the secondary tiles? AND Line 86, I am not clear on the use of the phrase "transition rates". Maybe specifying them as temporal transitions would be helpful.**

We have expanded the model description to clarify the tiling structure of LM3 and the representation of land-use change.

In LM3, land surface heterogeneity is represented using a sub-grid mosaic of tiles [Shevliakova et al., 2009, Malyshev et al., 2015] as illustrated in Fig. 1. Each tile has distinct energy and moisture balances for a vegetation–snow–soil column, biophysical properties, and exchanges of radiant and turbulent fluxes with the overlying atmosphere. LM3 predicts physical, biogeochemical, and ecological characteristics for each sub-grid land surface tile from the top of the vegetation canopy to the bottom of the soil column including leaves and canopy temperature, canopy-air specific humidity, stomatal conductance, snow cover and depth, runoff, vertical distribution of soil moisture, ice, and temperature. The land-use history is prescribed from the Hurtt et al. [2011] reconstruction for each grid cell in terms of annual transition rates among four distinct land-use types: undisturbed (hereafter referred to as natural), crops, pastures, and secondary vegetation. Secondary vegetation is defined in LM3 as the vegetation recovering after land-uses and land-cover changes and not currently managed. This includes all abandoned agricultural land as well as the land where wood was harvested at least once in prior years. The model keeps track of different recovery states by creating a secondary vegetation tile every time a disturbance occurs and simulation the subsequent vegetation regrowth in the tile. To avoid unrestricted growth of the number of tiles, the number of secondary vegetation tiles is limited to 10 per grid cell in the configuration of LM3 used here. When more than 10 secondary vegetation titles exist in a grid cell, secondary vegetation tiles with similar properties are merged [Shevliakova et al., 2009], while preserving water, energy, and carbon balances. Land properties that affect the surface removal of chemical tracers, such as snow cover, canopy wetness, surface and canopy temperature, leaf area index (LAI), stomatal conductance, and vegetation height are all prognostic [Shevliakova et al., 2009].

7. **Line 93: LAI is a critical parameter for deposition. Please provide more details on how this is determined.**
   We have added the following text:

   Vegetation carbon is partitioned into five pools: leaves, fine roots, sapwood, heartwood, and labile storage. The model simulates changes in vegetation and soil carbon pools, as well as the carbon exchange among these pools and the atmosphere. The sizes of the pools are modified daily depending on the carbon uptake and according to a set of allocation rules. Additionally, the model simulates changes in the vegetation carbon pools due to phenological processes, natural mortality, and fire. LAI is determined by vegetation leaf biomass and specific leaf area, prescribed for each vegetation type described below.

8. **Line 96: Do the management practices influence the agricultural emissions as well?**
   No, agricultural emissions are taken directly from HTAPv2 or CMIP5 estimates. We have added the following the text:

   The impact of management practices on the timing and magnitude of agricultural emissions (e.g., Paulot et al. [2014]) is not accounted for in AM3-LM3-DD.

9. **Line 101: What is the basis for your assumption that 25% of the leaf biomass is removed daily by grazing**

   We assume a high grazing intensity to prevent excessive accumulation of the biomass on pastures and the consequent misclassification of vegetation types on pasture as forests. This high grazing intensity does not lead to excessive overgrazing on pastures since no grazing occurs once pasture LAI drops below a prescribed limit (LAI=2 in our simulations). As a result, the long-term average rate of grazing is to the rate of growth of leaf biomass for the pastures where LAI is higher than 2.

10. **Lines 102-103: Does LM3 include a tree growth model? How does changing the grazing frequency affect the growth of trees? Also, at line 103, the text is a bit garbled**

    LM3 includes a fully prognostic dynamic vegetation model, and as such it does simulate the growth of vegetation, including trees. To clarify this point, we modified the text as follows:

Each vegetated tile has a unique vegetation type (C3 grass, C4 grass, temperate deciduous, coniferous, or tropical vegetation), which is determined based on biogeographical rules that take into account environmental conditions as well as current state of the vegetation in each tile [Shevliakova et al., 2009].

We also clarified the effects of the grazing on the growth of vegetation, and therefore on the vegetation types that the model simulates for pasture types:

This higher grazing frequency and intensity prevent the excessive growth of vegetation biomass on pastures in the tropics and mid latitudes, a problem which was noted in previous versions of LM3 [Malyshev et al., 2015] leading to misclassification of pasture vegetation cover as forests.

11. **Lines 112-113: It would be helpful to provide the equations for Rac in this manuscript. The Bonan (1996) reference is not readily available and is not as commonly used at the Erisman approach.**

    We have added the equation for both $R_{ac,v}$ and $R_{ac,g}$ to the text

$$R_{ac,g} = \frac{u_\star}{14(LAI + SAI)h} \tag{1}$$

$$R_{ac,v} = (LAI + SAI) \cdot g_b \text{ with } g_b = 0.01(1 - exp(-3/2)/3)\sqrt{\mathrm{V}} \tag{2}$$

    where SAI, h, and V are the stem area index, the height of the vegetation, and the normalized wind at the top of the canopy, respectively.

12. **Line 118: The leaf width is specified as one value for the land use type, while it is actually far more variable. How were the values in Table S1 determined? What is the sensitivity of the model to this parameter?**
    The values are taken from [Petroff and Zhang, 2010] (reference given in Table S1). $R_{b,v}$ scales like $lw^{1/3}$, therefore only large differences in leaf width (e.g., between coniferous and decidious) will significant modify $R_{b,v}$.

13. **Line 119: Insert species X here and other places.**
    corrected

14. **Line 127: A right parenthesis is missing.**
    corrected

15. **Line 129: After Rs(H2O), I suggest adding "is the stomatal resistance for water vapor" before "s calculated"**
    corrected

16. **Line 130-132: Water stress is included in most Jarvis based approaches which are commonly used in atmospheric chemistry models.**
    we have removed this statement

17. **Line 137: The notation in Table S1 does not match the table in the manuscript. How are the scaling factors for stem/bark determined?**

    thank you for noting this inconsistency. The notation used in Table S1 has been revised to match that used in the text. We use the estimate of Padro et al. [1993] for SO_2. We assume that $R_{sf,s}(O_3)/R_{sf,s}(SO_2)$ is the same as $R_{sf,v}(O_3)/R_{sf,v}(SO_2)$ in pasture. This has been clarified in the notes associated with Table S1.

18. **Lines 142-146: Please explain the nature of the modifications made to the original parameterization and how they were developed/evaluated.**

    Both the parameterization of Massad et al. [2010] and Simpson et al. [2003] rely on the surface concentrations of ammonia and acids to estimate the acidity of the surface. We find that this can create unrealistic oscillations in v_d(NH3) and $v_d(SO_2)$. This issue can be limited by using the 24h-integrated dry deposition fluxes instead. The text as been modified as follows:

To improve numerical stability, we estimate the acid ratio (r_{SN}) using the ratio of the 24-hour integrated total dry deposition of acids to the dry deposition of ammonia and ammonium, rather than using the ratio of their surface concentrations [Massad et al., 2010, Simpson et al., 2003].

19. **Lines 148-165: The motivation for this section is not clear. Since you are only comparing between models, it is not an evaluation.**
This now serves as preamble to the evaluation section.

20. **Section 2.2 It would be helpful to include information about all model runs in this section. Later in the paper, several new runs are described that are not included here. It would also be helpful to include a table that summarizes the important options used in the model runs. This could be included in the SI. What land use was used for the present day runs? Was there a spin-up year as was done for the future scenario run? What do you mean by across configurations at line 170? Were the emissions year specific? What year was used for the NH3 emissions that were used for the future scenario?**

We have given an ID to each simulation and we have also added a Table (Table 1) to summarize the different model configurations. Section 2.2 was rewritten as follows.

We perform two sets of global simulations representative of present-day (circa 2010) and future (2050) conditions. For present-day conditions, AM3-LM3-DD is run from 2007 to 2010 using 2007 as spin-up. The model is forced with observed sea surface temperatures and sea ice cover, and land use from the Representative Concentration Pathways 8.5 scenario (RCP8.5, Riahi et al. [2011]). Anthropogenic emissions are from the Hemispheric Transport of Air Pollution 2 (HTAPv2, Janssens-Maenhout et al. [2015]). Natural emissions are based on Naik et al. [2013], except for isoprene emissions, which are calculated interactively using the Model of Emissions of Gases and Aerosols from Nature (MEGAN, Guenther et al. [2006]). This simulation will be referred to as R2010 hereafter. An additional sensitivity experiment is performed (R2010_no_lu) with no anthropogenic land-use change, which is achieved by removing all vegetated tiles but the natural ones (expanding the area of the natural tiles). In both experiments, horizontal winds are nudged to those from the National Centers for Environmental Prediction reanalysis [Kalnay et al., 1996] to minimize meteorological variability between R2010 and R2010_no_lu.

For 2050, we use the vegetation, sea surface temperatures, and sea ice cover simulated by the GFDL-CM3 model under the RCP8.5 scenario in 2050 [Levy et al., 2013]. RCP8.5 anthropogenic emissions for 2050 are used [Lamarque et al., 2011] except for NH_3, where we use the spatial distribution and seasonality of HTAPv2 emissions following Paulot et al. [2016]. The model is run for 10 years with land-use fixed to year 2050 and we use the average of the last 9 years to minimize the impact of internal variability. This simulation will be referred to as R2050 hereafter. We perform two additional sensitivity experiments to characterize how land-use change (R2050_2010lu) and climate (R2050_2010climate) contribute to the change in deposition velocity between R2010 and R2050. The different model runs are summarized in Table 1

21. ***Section 2.3 (to be added) There should be a section that describes the observational data used. How did you choose which ones to include? It might be helpful to include a table of the observational data to reduce the amount of text needed in the legend in Figure 3.***

We performed a litterature survey to identify observations of $v_d(SO_2)$ over a wide range of environments. We have added a table in the supplementary materials (Table S3), summarizing the observations. The text was revised as follows:

We first evaluate the simulated $v_d(SO_2)$ in AM3-LM3–DD for present-day (2007-2010) against observations collected over a wide range of surfaces (Table S3). We sample the simulated monthly diurnal cycle of $v_d(SO_2)$ at the location of the measurements in the tile that best represents the type of vegetation reported in the observations. We further distinguish between day-time (8am-5pm) and night-time (10pm-4am) samples and wet (wet fraction of the canopy greater than 10%) and dry periods.

22. **Lines 181-190: There is a lot more analysis that could be done in this section. For example, the differences in performance between land use types could be expanded. Are there aspects of the model that you think contribute to these differences? Canopy wetness is very important**

to SO2 deposition. How well does the model capture wetness compared to the observations?

We find that AM3-LM3-DD falls within a factor of two of most observations. This is consistent with the uncertainty reported by Wu et al. [2018] for state of the art dry deposition models. We have expanded the analysis of the model biases as follows:
Simulated deposition velocities generally fall within a factor of 2 of the observations, with better agreement during the day than at night, when the model is biased high. This uncertainty range is similar to the one reported by Wu et al. [2018] for a range of dry deposition models. More specifically, AM3-LM3-DD qualitatively captures the range of deposition velocities over forested ecosystems, including the slower deposition of SO_2 *in winter than in summer and under dry than under wet conditions in deciduous forests and the fast removal of* SO_2 *over coniferous forests. However, the model fails to capture the elevated* $v_d(SO_2)$ *(>1 cm/s) reported by several studies over grassland. This may reflect uncertainties in the representation of ammonia emissions (e.g., no sub-grid heterogeneity), which could result in an underestimate of* SO_2-NH_3 *co-deposition over crops or fertilized grasslands [Nemitz et al., 2001, Flechard et al., 2013].*

We have also clarified how the canopy wetness is estimated. The following text was added to the method section:

The fraction of the canopy covered by liquid water (f_l) and snow (f_s) are estimated from the intercepted canopy liquid water mass (w_l) and snow mass (w_s) following Bonan [1996]:

$$f_i = \left(\frac{w_i}{W_{i,max}}\right)^{\frac{2}{3}} \qquad i \in \{l, s\} \tag{3}$$

where $W_{l,max} = 0.02 kg\,m^{-2}$ *and* $W_{s,max} = 0.2 kg\,m^{-2}$ *are the maximum liquid water and snow holding capacities, respectively. If both snow and liquid water are present simultaneously, water and snow are assumed to be distributed independently of each others.*

Fig. 2 shows that AM3-LM3-DD captures the qualitative impact of canopy wetness on $v_d(SO_2)$. However, we agree with the reviewer that the treatment of canopy wetness and its impact on deposition velocities remain important uncertainties in current models. This has been emphasized in the conclusion, as follows:

Our study highlights the importance of accounting for surface heterogeneities and anthropogenic land use in modulating the magnitude and trend of N deposition. Here, we leverage the tiled structure of the GFDL land model to efficiently represent the subgrid scale heterogeneity of surface properties and their evolution in a changing climate. We have shown that the shift of N emissions from oxidized to reduced N in North America will exacerbate the sensitivity of N deposition to small-scale heterogeneities, which highlights the need to improve the representation of non-stomatal surface resistances ($R_{sf,v}$, $R_{sf,s}$, and $R_{sf,g}$) including their modulation by canopy wetness and acidity [Flechard et al., 2013, Wentworth et al., 2016, Wu et al., 2018].

23. **Lines 191-213: This section mostly describes model development as the text describes how observations of deposition velocity were used to develop the alpha and beta parameters for equation 6. It is not clear how the MERRA meteorological fields were included in the modeling. At line 200, reiterate that the measured compounds are those from Nguyen et al. At line 203, it would be appropriate to refer the reader back to Figure 4. How do you know what the deposition of HCN on cuticles is or are you referring to how the model treats the deposition?**

We use MERRA meteorological fields to drive LM3 (instead of AM3 simulated fields), as it allows to better capture meteorological condition at the SOAS site. The text was modified as follows:

To facilitate the comparison between simulated and observed deposition velocities, we use meteorological fields (wind speed, temperature, precipitation, and downward radiation) from the Modern-Era Retrospective Analysis

for Research and Applications (MERRA) [Rienecker et al., 2011] to drive a standalone version of LM3-DD. This provides a more accurate representation of the site conditions than using meteorological fields simulated by AM3.

HCN is poorly soluble and does not exhibit significant reactivity at the leaf surface [Nguyen et al., 2015]. This was clarified as follows:

In contrast, the low solubility and low reactivity at the leaf surface of HCN produces a large non stomatal resistance [Nguyen et al., 2015] ($R_{sf,v} >>> 1$ s/m), such that $v_d(\mathrm{HCN}) \simeq R_s(\mathrm{HCN})^{-1}$.

24. **Line 220: Note that the model captures the high reduced N over NC.**

The text has been modified as follows:

with high deposition in the Northeast and greater contribution of reduced nitrogen to N deposition in the US Midwest and North Carolina than in the Eastern US.

25. ***Line 222: In Figure 5 (middle column), what causes the streak pattern in the middle of the country?***

This reflects the large difference in vegetation height between the actual vegetation height and that of natural vegetation.

The text was revised as follows:
This enhancement is largest in regions where land-use change has caused a large decrease in vegetation height and LAI (e.g., in the US Midwest and Northeast, Fig. S2) and smallest in regions with little agricultural activity (e.g., most of Canada) or where managed vegetation differs little in height and LAI from natural vegetation (e.g., in the Western US, Fig. S2).

Fig. S2 shows the difference in vegetation height and LAI associated with land-use change.

26. **Line 223-224: The text that appears at line 229-230 would be better placed here rather than simply referring vaguely to the supplementary materials.**

We are now referring to Fig. S1

27. **Line 228: The land use is not actually changing in this analysis. Do you mean the the dry deposition of NHx would be more sensitive?**
We have modified the text as follows:
... also shows that the dry deposition of NH_x exhibits a greater enhancement over natural vegetation than the dry deposition of NO_y, consistent with the greater sensitivity of $v_d(\mathrm{NH_3})$ than $v_d(\mathrm{HNO_3})$ to surface properties (Fig. S3).

28. **Line 235: What are you contrasting?**
We have removed *In contrast.*

29. **Line 240-241: This model run should be discussed in the methods section. How was this done in the model? Changes in the land use would also change the meteorology and the emissions. Were these considered?**

The effect of land-use on meteorology is limited by nudging the horizontal wind speeds to those from NCEP and prescribing the sea surface temperature and sea ice. This has been clarified in the method section (see reply to comment 20)

30. **Line 241: It would be helpful to insert text along the lines of "Using this run as the base case, we compare . . ." That would fit better with the text later in the section that compares the impact of anthropogenic land use changes.**

The text was modified as follows:
Fig. 6 shows the change in dry NO_y, dry NH_x, and total N deposition associated with anthropogenic land-use change, which is estimated by comparing R2010 and R2010_no_lu. We find that anthropogenic land-use

change reduces dry NO_y*, dry* NH_x*, and total N deposition over the contiguous US by 8%, 26%, and 6%, respectively. The reduction in N deposition associated with anthropogenic land-use change is largest in the Central and Eastern US, where deforestation has caused a large reduction in LAI and vegetation height (Fig. S4).*

31. **Lines 254-256: Were changes in biogenic and agricultural emissions considered?**

    Emissions are either calculated (e.g., for isoprene) or read from monthly files on the atmospheric side and are not calculated in LM3. This has been clarified in the method section as described in reply to comment 8 from reviewer 1.

32. **Line 257: What land use takes the place of agricultural areas in the scenario?**

    Only natural vegetation, glacier, and water tiles are considered in this simulation. This has been clarified in the revised experimental design (see reply to comment 20)

33. **Line 258-260: This section needs more explanation.**

    We have revised the text as follows:

    We find a small increase (<10%) in the deposition velocity of HNO_3 *over most of the US between R2050 and R2010 (Fig. S4). This is attributed to a reduction in the land fraction devoted to agriculture between 2010 and 2050 in the RCP8.5 [Davies-Barnard et al., 2014], which results in taller vegetation and higher LAI. The impact of this change in land use between 2010 and 2050 is larger for* $v_d(NH_3)$*, which increases by more >10% over most of the Midwest and Eastern US. However, in the Eastern US and US Midwest, this increase is more than compensated by a reduction in acid deposition, which results in an overall decrease of* $v_d(NH_3)$ *of 10 to 20% over most of the Eastern US. This highlights the need to better characterize the impact of the co-deposition of acids and ammonia on the removal of ammonia to improve projection of future N deposition.*

34. **Line 270: Suggest adding "to natural vegetation from 2010-2050" after N deposition.**
    done

35. **Line 273: Suggest adding "for the grid" after deposition.**
    done

36. **Figure 3: What is the time scale for each point – e.g. monthly average? It isn't clear what you mean by "the model is sampled". The legend is far too small to be read easily. Perhaps some of the information could be included in a table. Some of the colors are hard to see or distinguish. The yellow doesn't show up at all in print and the blues are hard to distinguish. The symbols are small which makes it hard to tell them apart. Explain the symbol fill similar to how the shape is explained. How was the criteria for wet conditions determined? This could be explained in the methods section when you add a section for the observational data.**

    We have revised Fig. 4 following the comments of both reviewers 1 and 2 and expanded both the figure's caption and associated method section. See reply to comment 21.

37. **Figure 4: It would be helpful to have H2O2 and HNO3 on the same scale since these are compared in the manuscript. The surfaces listed are not consistent with the main text. Bark is listed rather than stem.**

    we have revised the figure following the reviewer's suggestion.

2 Reviewer 2

1. **The Introduction could be extended with a short overview of what has been done sofar regarding subgrid variations in deposition.**

We have added the following text to the introduction:

Significant challenges remain in quantifying the long-term impacts of N deposition on ecosystems in a changing climate [Sutton et al., 2008, Wu and Driscoll, 2010, Phoenix et al., 2012, Högberg, 2012, de Vries et al., 2015, Storkey et al., 2015], including uncertainties in the speciation, magnitude and spatial distribution of the N deposition flux itself [Sutton et al., 2008, Ochoa-Hueso et al., 2011, Jickells et al., 2013, Fleischer et al., 2013]. Many approaches have been developed to provide high-resolution, ecosystem-relevant estimates of both wet and dry N deposition, including statistical models [Singles et al., 1998, Dore et al., 2007, Weathers et al., 2006, Dore et al., 2012], high-resolution nested chemical transport model ($\simeq 4 \times 4\,km$ [Vieno et al., 2009, Simkin et al., 2016]), and hybrid approaches that combine high-resolution regional chemical transport models with observed N fluxes and atmospheric concentrations (e.g. using the Community Multiscale Air Quality Modeling System [Schwede and Lear, 2014, Bytnerowicz et al., 2015, Williams et al., 2017]). However, the elevated computational requirement associated with high-resolution atmospheric models make such approaches impractical for assessing the long-term impact of N deposition on ecosystems, its sensitivity to climate change, and ultimately its coupling with the carbon cycle [Smith et al., 2014, Zaehle et al., 2010, Fleischer et al., 2013, Dirnböck et al., 2017, Fleischer et al., 2015]. For such questions, estimates of N deposition are generally derived from global models with coarse resolution ($\simeq$ 100km, [Dentener et al., 2006, Lamarque et al., 2013]). This introduces a large uncertainty [Hertel, 2011] in N deposition estimates especially for dry deposition, which can vary over short distances ($\sim$1 km) in response to changes in the physical, hydrological, and ecological state of the surface [Weathers et al., 2000, Hicks, 2006, 2008, De Schrijver et al., 2008, Ponette-González et al., 2010, Templer et al., 2014, Tulloss and Cadenasso, 2015].

2. **Could the authors add another short section about the observations that are used to validate the modelled Vds? The comparison between measurements and model results is difficult to interpret without this information.**

   We have split the model evaluation section into two sub sections. We have added a table summarizing the observation shown in Fig. 2 in the supplementary materials. See replies to comments 21 and 22 from reviewer 1.

3. **Section 2.1: Figure 2 and its interpretation seems dislocated and should be part of the Result section.**

   This section was moved to the evaluation section.

4. **Section 2.1: for NH3 the bi-directional flux using compensation point modelling is essential to model NH3 fluxes. Furthermore, for agricultural lands fertilization rates are important to determine the net flux of NH3.**

   The current representation of agriculture in LM3 is not sufficiently detailed to represent the bidirectional exchange. This has been clarified in the model description section in addition to the conclusion (see reply to comment 1 from reviewer 1).

   We have further noted that the bidirectional nature of ammonia exchange should increase the enhancement of NHx deposition relative to the grid-box average. The text was modified as follows:

   The enhancements of the dry deposition of NH_x *over natural vegetation is likely to be underestimated by AM3-LM3-DD as the surface bidirectional exchange of* NH_3 *tends to reduce its deposition in source regions.*

5. **The Experimental section does not include all the steps that are taken. It would help if the authors would explain in detail what their approach was.**

   We have revised the experimental section according to comments from both reviewers 1 and 2 (see reply to comment 20 from reviewer 1). We have also added a table to the main text (Table 1), which summarizes the different model configurations used in this study.

6. **I would suggest to split up section 3.2. into two different sections: one section where Figure 5 is discussed and one that discusses the land use specific changes (Figure 6). I suggest to also split up section 3.3. One section that discusses the relative changes of anthropogenic land use changes on oxidized/reduced/total N deposition, and one about the contribution of natural**

land and water bodies to the total change in Nr deposition.

Thank you. We have followed the reviewer's suggestion for section 3.2 that we have expanded. For section 3.3, we think it's clearer not to split the discussion of Fig. 7.

7. **Figure 4 shows clear overestimation during nighttime and at the end of the day. Could the authors discuss this, also in relation to the conclusions they draw from the comparison in Figure 4?**

   The overestimate is found for all species but HCN. Because H2O2 and HNO3 have little surface resistance, we hypothesize that the overestimate is associated with insufficient aerodynamic resistance at night. The text is modified as follows:
   Finally, we note that the comparison against SOAS observations points to a significant high bias in simulated night-time deposition velocity. Since this bias is found for all species including $v_d(H_2O_2)$ and $v_d(HNO_3)$, this suggests that the model underestimates the aerodynamic resistance (R_a) during these periods.

8. **Can the authors elaborate on the land use changes that are used in the model? What are for instance the regions where we see the largest changes?**

   We have added a figure in the supplementary materials that shows the change in LAI and vegetation height associated with land-use change (Fig. S2). We have also clarified how land-use change is implemented in LM3 in the method section as follows:
   The land-use history is prescribed from the Hurtt et al. [2011] reconstruction for each grid cell in terms of annual transition rates among four distinct land-use types: undisturbed (hereafter referred to as natural), crops, pastures, and secondary vegetation. Secondary vegetation is defined in LM3 as the vegetation recovering after land-uses and land-cover changes and not currently managed. This includes all abandoned agricultural land as well as the land where wood was harvested at least once in prior years. The model keeps track of different recovery states by creating a secondary vegetation tile every time a disturbance occurs and simulation the subsequent vegetation regrowth in the tile. To avoid unrestricted growth of the number of tiles, the number of secondary vegetation tiles is limited to 10 per grid cell in the configuration of LM3 used here. When more than 10 secondary vegetation titles exist in a grid cell, secondary vegetation tiles with similar properties are merged [Shevliakova et al., 2009], while preserving water, energy, and carbon balances.

9. **Could the authors elaborate a bit more on how the changes in N deposition in natural parks (mentioned at the end of section 3.3) are computed? Did the authors assume that the national parks cover an entire grid cell or did they for instance use a mask on the level of the land model?**

   We use N deposition to natural vegetation as a proxy for N deposition to natural parks. This has been clarified as follows:

   Fig. 5 shows that it has important implications for N deposition at national parks, which are best represented by natural vegetation tiles.

10. **Detailed remarks: Page 3 line 80-82: this seems obvious. However, can the authors give examples where a comprehensive land model is included or at least a zooming option?**

    We are not aware that other global climate models have used such zooming options. As noted in reply to comment 1, we have expanded the introduction to highlight ongoing efforts to improve estimates of present-day N deposition.

11. **Page 3 line 88: can the authors explain a little more about the tiles sizes and its use in the mosaic approach, including information about the gridcell sizes?**

    Please see reply to comment 6 from reviewer 1. Fig. S1 also shows the tile size for natural and water bodies in LM3.

12. **Page 4 line 104: management practices are important, but that also holds for fertilization.**

    We agree with the reviewer. Howevever LM3 does not yet include a detailed treatment of agricultural activities. In other words, the cropping schedule does not affect ammonia emissions, which are prescribed on the atmospheric side.

13. **Page 4 line 109: 25% of biomass removed during grazing seems too high. Do the authors have a reference?**

    see reply to comment 9 from reviewer 1

14. **Page 4 line 112 – for crops, the representation of management practices needs some more explanation. Could you elaborate on how the planting and harvesting dates were determined?**

    For planting and harvesting, we use a climatology [Portmann et al., 2010]. We have clarified that LM3 does not calculate cropping schedule (e.g., [Bondeau et al., 2007]), as follows:

    LM3 does not estimate the cropping schedule (e.g., Bondeau et al. [2007]) and we specify planting and harvesting dates from the global monthly irrigated and rainfed crop areas climatology [Portmann et al., 2010].

15. **Page 6 line 158 – I suggest to move the comparison of Vd from different models (the part related to Fig 2.) to the results and discussion section.**

    We have moved this section to the evaluation section

16. **Page 6 Figure 3: it is not clear how the simulation was done: same locations? Actual meteorology or modelled? Surface characteristics?**

    We have clarified how the comparison was performed as follows:
    We first evaluate the simulated present-day (R2010) $v_d(SO_2)$ against observations collected over a wide range of surfaces (Table S3). We sample the simulated monthly diurnal cycle of $v_d(SO_2)$ at the location of the measurements in the tile that best represents the type of vegetation reported in the observations. We further distinguish between day-time (8am-5pm) and night-time (10pm-4am) samples and wet (wet fraction of the canopy greater than 10%) and dry periods.

17. **Page 7 – line 192 – I suggest to change the title 'Evaluation' into something more specific (for instance 'Evaluation of model Vd against observations', or something on that line). The beginning of this sections should be moved to the experimental description.**

    We have revised the title for this section as suggested by the reviewer. We have kept the description of the standalone LM3 configuration in this section as it is not used elsewhere.

18. **Figure 5 – could the authors add the time period of the simulations to the description of the figure, so that it is self-explanatory. The titles 'All land' are a bit vague, maybe it is better to use 'All land types' or something in that direction. How many observations were used? Furthermore, can the authors explain the pattern in nitrogen deposition in central US, which is clear in the middle part (natural/all land)?**

    We have revised Fig.5 (and Fig. 7) as suggested by the reviewer. The large enhancement of N deposition in the central US over natural vegetation reflects the higher vegetation height of natural vegetation relative to the average vegetation height across all land types.

    The text was revised as follows:
    This enhancement is largest in regions where land-use change has caused a large decrease in vegetation height and LAI (e.g., in the US Midwest and Northeast, Fig. S2) and smallest in regions with little agricultural activity (e.g., most of Canada) or where managed vegetation differs little in height and LAI from natural vegetation (e.g., in the Western US, Fig. S2).

    Fig. S2 shows the difference in vegetation height and LAI associated with land-use change.

19. **Page 8 line 237 – How would fertilization raters and the bi-directional nature of the NH3 flux influence the results in areas near to agricultural regions?**

    We expect that the simulated enhancement of N deposition over natural tiles relative to the average deposition over all land tiles may be an underestimate. This has been clarified in the analysis of the results as follows:
    The enhancements of the dry deposition of NH_x over natural vegetation is likely to be underestimated in AM3-LM3-DD as the surface bidirectional exchange of NH_3 tends to reduce its deposition in source regions.

20. **Figure 6 – all the numbers that are mentioned on the sides of the figure are a bit hard to follow. Please consider presenting the number in a different way.**

We have made the text much larger. We have also moved the fractional change in N deposition over the contiguous US to the text.

21. **Figure 7 same as Figure 6.**

see reply to previous comment

3 Reviewer 3

1. **Based on the discussions in Section 3.1, I feel that the modelled Vd used in this study may be biased higher, or at least among the upper-end range of existing models such as those shown in Wu et al. (2018). Very high Vd values for some of the N species measured in Nguyen et al., 2015 are close to or even higher than the maximum possible Vd controlled by aerodynamic and sublayer resistances, and cannot be reproduced by the existing dry deposition models even after adjusting model parameters to the upper range of reasonable values. To avoid too much overestimation of dry deposition, these values are not recommended to be generalized to other regions before more measurement evidences become available. As for the present study, I understand the typical magnitude of uncertainties in dry deposition estimation is about a factor of 2 (Wu et al., 2018), and such uncertainties should be included in the discussion of modeled results and associated impacts on ecosystem health assessment. A brief discussion and recommendation related to this issue may be helpful to readers.**

We agree with the reviewer that more measurements are needed to better constrain the deposition velocity of organic nitrate. We have added the following text:

We find that ($\alpha = 7$, $\beta = 1$) provide a reasonable fit for all organic nitrates. These parameters imply that the deposition of isoprene-derived organic nitrates is primarily controlled by dry cuticles with small contributions of stomata and stems. We note that these parameters imply a much greater solubility and reactivity of organic nitrogen than in other models (e.g., $\alpha = 0$, $\beta = 0.5$ in AURAMS [Zhang et al., 2002]). While we use these parameters globally, such large differences warrant further investigations, as the deposition of organic nitrogen may account for over 25% of the overall N deposition but remains rarely measured [Jickells et al., 2013].

In the section *Evaluation of simulated* v_d *against observations*, we are now referring to the study by Wu et al. [2018] as follows:

The resistance approach implemented in AM3-LM3-DD is similar to that used in most chemical transport models and has been evaluated extensively. However differences in implementations can result in large differences between simulated deposition velocities [Wu et al., 2018].

This has been further emphasized in the conclusion:
We have shown that the shift of N emissions from oxidized to reduced N in North America will exacerbate the sensitivity of N deposition to small-scale heterogeneities, which highlights the need to improve the representation of non-stomatal surface resistances ($R_{sf,v}$, $R_{sf,s}$, and $R_{sf,g}$) including their modulation by canopy wetness and acidity [Flechard et al., 2013, Wentworth et al., 2016, Wu et al., 2018].

2. **A related point to the above comment: I noticed that the other two reviewers both recommended using the bi-directional approach for NH3 deposition. I agree this approach is better in theory, but may not be practical in global models with the current limited knowledge of emission potentials in various land uses. I feel that using unidirectional depositional approach for NH3 is still acceptable if the chosen dry deposition model provides conservative Vd for NH3 (which compensates some of the bidirectional fluxes). Under such a condition, the NH3 deposition estimates would be valid for non-fertilized land use types and would represent the upper-end estimates for agricultural areas. This point can be made in the revised paper.**

We agree with the reviewer that the bidirectional exchange remains challenging to incorporate in global climate models. In addition to uncertainties in the NH3 emission potential of different vegetation types, the representation agricultural activities in LM3 (and many other global dynamic vegetation models) remains insufficient to represent ammonia emissions.
We have added the following text to the method section:
The bidirectional exchange of ammonia is not represented in AM3-LM3-DD [Massad et al., 2010, Flechard et al., 2013]. This reflects in part uncertainties in the emission potential of vegetation and the lack of detailed treatment of agricultural activities in LM3 [Riddick et al., 2016]. We thus expect AM3-LM3-DD to overestimate NH_3 *dry deposition in source regions [Zhu et al., 2015, Sutton et al., 2007].*

Table 1: Model runs

Run ID	Climate	Land Use	Anthropogenic Emissions
R2010	2008–2010[a]	RCP8.5 (2008–2010)	HTAPv2
R2010_no_lu	2008–2010[a]	natural vegetation	HTAPv2
R2050	2050	RCP8.5 (2050)	RCP8.5 (2050)[b]
R2050_2010lu	2008–2010[a]	RCP8.5 (2008–2010)	RCP8.5 (2050)[b]
R2050_2010climate	2008–2010[a]	RCP8.5 (2050)	RCP8.5 (2050)[b]

[a] horizontal winds are nudged to NCEP

[b] with modified NH_3 emissions following Paulot et al. [2016]

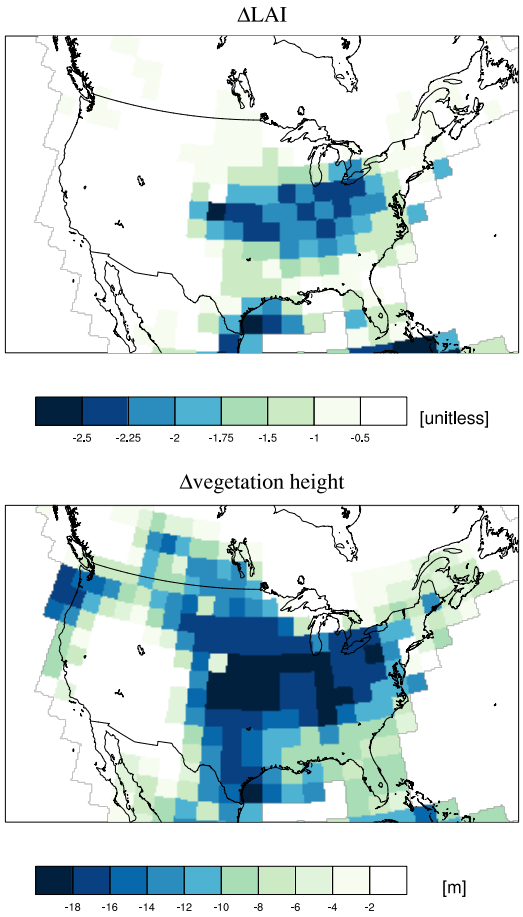

Figure S2: Overall change in LAI and vegetation height associated with anthropogenic land-use change (2008–2010 average)

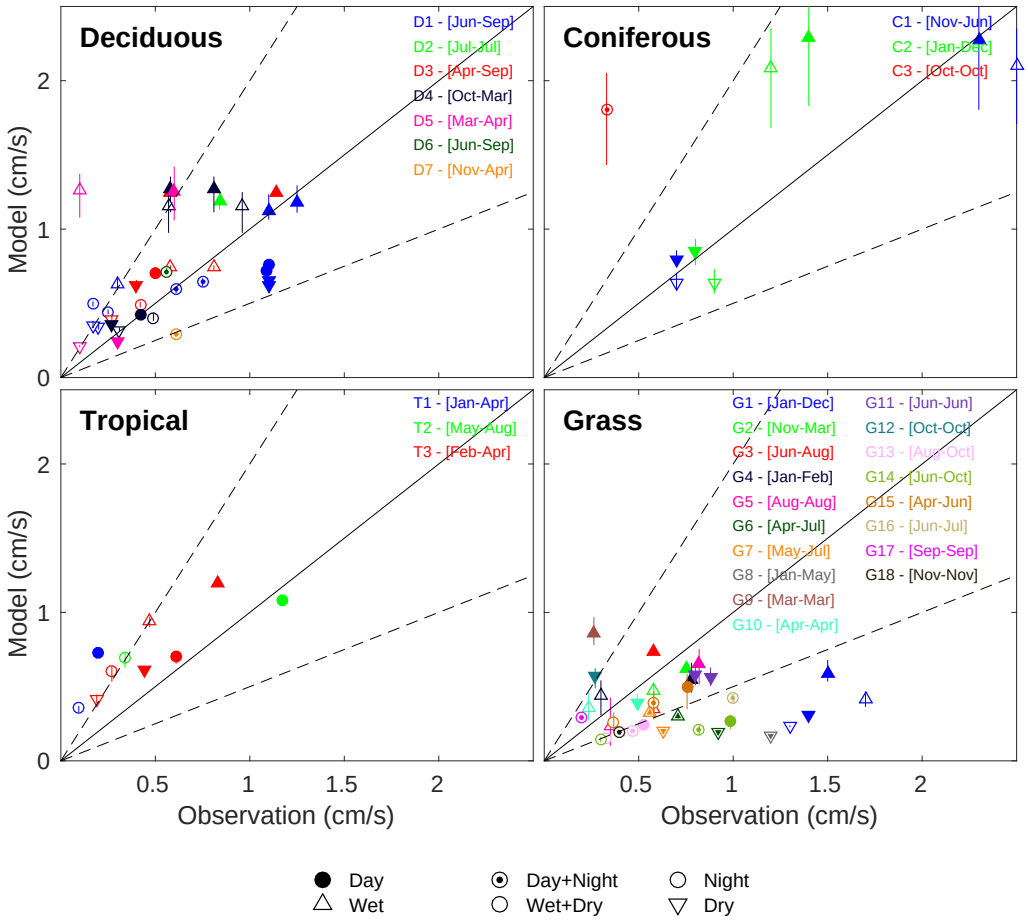

Figure 4: Observed and simulated deposition velocities of SO_2 for different vegetation types. The symbol shape indicates the canopy status: wet (upward pointing triangle), dry (downward point triangle), circle (average). The symbol fill indicates the time period: filled (day), half-filled (day+night), empty (night). The monthly diurnal cycle of deposition velocities simulated by AM3-LM3-DD (R2010 simulation) is sampled at each observation site in the tile that best represents the observed ecosystem accounting for the month, time of day and canopy wetness status when the observations were collected . References for the different sites are given in Table S3.

References

Gordon B Bonan. Land surface model (lsm version 1.0) for ecological, hydrological, and atmospheric studies: Technical description and users guide. technical note. Technical report, National Center for Atmospheric Research, Boulder, CO (United States). Climate and Global Dynamics Div., 1996.

A. Bondeau, P.C. Smith, S. Zaehle, S. Schaphoff, W. Lucht, W. Cramer, D. Gerten, H. Lotze-Campen, C. Müller, M. Reichstein, et al. Modelling the role of agriculture for the 20th century global terrestrial carbon balance. *Global Change Biol.*, 13(3):679–706, 2007.

A. Bytnerowicz, R.F. Johnson, L. Zhang, G.D. Jenerette, M.E. Fenn, S.L. Schilling, and I. Gonzalez-Fernandez. An empirical inferential method of estimating nitrogen deposition to mediterranean-type ecosystems: the san bernardino mountains case study. *Environmental Pollution*, 203:69–88, aug 2015. doi: 10.1016/j.envpol.2015.03.028. URL `https://doi.org/10.1016/j.envpol.2015.03.028`.

T. Davies-Barnard, P. J. Valdes, J. S. Singarayer, F. M. Pacifico, and C. D. Jones. Full effects of land use change in the representative concentration pathways. *Environ. Res. Lett.*, 9(11):114014, 2014. ISSN 1748-9326. doi: 10.1088/1748-9326/9/11/114014. URL `http://stacks.iop.org/1748-9326/9/i=11/a=114014`.

A. De Schrijver, J. Staelens, K. Wuyts, G. Van Hoydonck, N. Janssen, J. Mertens, L. Gielis, G. Geudens, L. Augusto, and K. Verheyen. Effect of vegetation type on throughfall deposition and seepage flux. *Environ. Pollut.*, 153(2): 295–303, May 2008. ISSN 0269-7491.

Wim de Vries, Jean-Paul Hettelingh, and Maximilian Posch, editors. *Critical Loads and Dynamic Risk Assessments*, volume 25 of *Environmental Pollution*. Springer Netherlands, Dordrecht, 2015. ISBN 978-94-017-9507-4 978-94-017-9508-1.

F. Dentener, J. Drevet, J. F. Lamarque, I. Bey, B. Eickhout, A. M. Fiore, D. Hauglustaine, L. W. Horowitz, M. Krol, U. C. Kulshrestha, M. Lawrence, C. Galy-Lacaux, S. Rast, D. Shindell, D. Stevenson, T. Van Noije, C. Atherton, N. Bell, D. Bergman, T. Butler, J. Cofala, B. Collins, R. Doherty, K. Ellingsen, J. Galloway, M. Gauss, V. Montanaro, J. F. Müller, G. Pitari, J. Rodriguez, M. Sanderson, F. Solmon, S. Strahan, M. Schultz, K. Sudo, S. Szopa, and O. Wild. Nitrogen and sulfur deposition on regional and global scales: A multimodel evaluation. *Global Biogeochem. Cycles*, 20:B4003, October 2006.

T. Dirnböck, C. Foldal, I. Djukic, J. Kobler, E. Haas, R. Kiese, and B. Kitzler. Historic nitrogen deposition determines future climate change effects on nitrogen retention in temperate forests. *Climatic Change*, 144(2): 221–235, jul 2017. doi: 10.1007/s10584-017-2024-y. URL `https://doi.org/10.1007/s10584-017-2024-y`.

A Dore, M Vieno, Y Tang, U Dragosits, A Dosio, K Weston, and M Sutton. Modelling the atmospheric transport and deposition of sulphur and nitrogen over the united kingdom and assessment of the influence of SO2 emissions from international shipping. *Atmospheric Environment*, 41(11):2355–2367, apr 2007. doi: 10.1016/j.atmosenv.2006.11.013. URL `https://doi.org/10.1016/j.atmosenv.2006.11.013`.

A. J. Dore, M. Kryza, J. R. Hall, S. Hallsworth, V. J. D. Keller, M. Vieno, and M. A. Sutton. The influence of model grid resolution on estimation of national scale nitrogen deposition and exceedance of critical loads. *Biogeosciences*, 9(5):1597–1609, may 2012. doi: 10.5194/bg-9-1597-2012. URL `https://doi.org/10.5194/bg-9-1597-2012`.

C. R. Flechard, R.-S. Massad, B. Loubet, E. Personne, D. Simpson, J. O. Bash, E. J. Cooter, E. Nemitz, and M. A. Sutton. Advances in understanding, models and parameterizations of biosphere-atmosphere ammonia exchange. *Biogeosciences*, 10(7):5183–5225, July 2013. ISSN 1726-4189.

K. Fleischer, K. T. Rebel, M. K. van der Molen, J. W. Erisman, M. J. Wassen, E. E. van Loon, L. Montagnani, C. M. Gough, M. Herbst, I. A. Janssens, D. Gianelle, and A. J. Dolman. The contribution of nitrogen deposition to the photosynthetic capacity of forests. *Global Biogeochem. Cycles*, 27(1):187–199, March 2013. ISSN 1944-9224.

K. Fleischer, D. Wårlind, M. K. van der Molen, K. T. Rebel, A. Arneth, J. W. Erisman, M. J. Wassen, B. Smith, C. M. Gough, H. A. Margolis, A. Cescatti, L. Montagnani, A. Arain, and A. J. Dolman. Low historical nitrogen deposition effect on carbon sequestration in the boreal zone. *J. Geophys. Res. Biogeosci.*, 120(12):2015JG002988, December 2015. ISSN 2169-8961.

A. Guenther, T. Karl, P. Harley, C. Wiedinmyer, P. I. Palmer, and C. Geron. Estimates of global terrestrial isoprene emissions using MEGAN (Model of Emissions of Gases and Aerosols from Nature). *Atmos. Chem. Phys.*, 6(11): 3181–3210, 2006.

Ole Hertel. *The European Nitrogen Assessment: Sources, Effects and Policy Perspectives*, chapter 14. Cambridge University Press, May 2011. ISBN 1107006120.

Bruce B. Hicks. Dry deposition to forests—On the use of data from clearings. *Agric. For. Meteorol.*, 136(3–4):214–221, February 2006. ISSN 0168-1923. doi: 10.1016/j.agrformet.2004.06.013. URL `http://www.sciencedirect.com/science/article/pii/S0168192305002066`.

Bruce B. Hicks. On Estimating Dry Deposition Rates in Complex Terrain. *Journal of Applied Meteorology and Climatology*, 47(6):1651–1658, June 2008. ISSN 1558-8424.

Peter Högberg. What is the quantitative relation between nitrogen deposition and forest carbon sequestration? *Glob. Chang. Biol.*, 18(1):1–2, January 2012. ISSN 1365-2486.

G. C. Hurtt, L. P. Chini, S. Frolking, R. A. Betts, J. Feddema, G. Fischer, J. P. Fisk, K. Hibbard, R. A. Houghton, A. Janetos, C. D. Jones, G. Kindermann, T. Kinoshita, Kees Klein Goldewijk, K. Riahi, E. Shevliakova, S. Smith, E. Stehfest, A. Thomson, P. Thornton, D. P. van Vuuren, and Y. P. Wang. Harmonization of land-use scenarios for the period 1500–2100: 600 years of global gridded annual land-use transitions, wood harvest, and resulting secondary lands. *Clim. Change*, 109(1-2):117–161, November 2011. ISSN 0165-0009, 1573-1480.

G. Janssens-Maenhout, M. Crippa, D. Guizzardi, F. Dentener, M. Muntean, G. Pouliot, T. Keating, Q. Zhang, J. Kurokawa, R. Wankmüller, H. Denier van der Gon, J. J. P. Kuenen, Z. Klimont, G. Frost, S. Darras, B. Koffi, and M. Li. HTAP_v2.2: a mosaic of regional and global emission grid maps for 2008 and 2010 to study hemispheric transport of air pollution. *Atmos. Chem. Phys.*, 15(19):11411–11432, October 2015. ISSN 1680-7324. doi: 10.5194/acp-15-11411-2015. URL `http://www.atmos-chem-phys.net/15/11411/2015/`.

T. Jickells, A. R. Baker, J. N. Cape, S. E. Cornell, and E. Nemitz. The cycling of organic nitrogen through the atmosphere. *Philos. Trans. R. Soc. London, Ser. B*, 368(1621), July 2013. ISSN 0962-8436, 1471-2970. PMID: 23713115.

E. Kalnay, M. Kanamitsu, R. Kistler, W. Collins, D. Deaven, L. Gandin, M. Iredell, S. Saha, G. White, J. Woollen, Y. Zhu, A. Leetmaa, R. Reynolds, M. Chelliah, W. Ebisuzaki, W. Higgins, J. Janowiak, K. C. Mo, C. Ropelewski, J. Wang, Roy Jenne, and Dennis Joseph. The NCEP/NCAR 40-Year Reanalysis Project. *Bull. Am. Meteorol. Soc.*, 77(3):437–471, March 1996. ISSN 0003-0007.

J.-F. Lamarque, F. Dentener, J. McConnell, C.-U. Ro, M. Shaw, R. Vet, D. Bergmann, P. Cameron-Smith, S. Dalsoren, R. Doherty, G. Faluvegi, S. J. Ghan, B. Josse, Y. H. Lee, I. A. MacKenzie, D. Plummer, D. T. Shindell, R. B. Skeie, D. S. Stevenson, S. Strode, G. Zeng, M. Curran, D. Dahl-Jensen, S. Das, D. Fritzsche, and M. Nolan. Multi-model mean nitrogen and sulfur deposition from the atmospheric chemistry and climate model intercomparison project (ACCMIP): evaluation of historical and projected future changes. *Atmos. Chem. Phys.*, 13(16): 7997–8018, August 2013. ISSN 1680-7324.

Jean-François Lamarque, G. Kyle, Malte Meinshausen, Keywan Riahi, Steven Smith, Detlef van Vuuren, Andrew Conley, and Francis Vitt. Global and regional evolution of short-lived radiatively-active gases and aerosols in the representative concentration pathways. *Clim. Change*, 109:191–212, 2011. ISSN 0165-0009. 10.1007/s10584-011-0155-0.

Hiram Levy, Larry W. Horowitz, M. Daniel Schwarzkopf, Yi Ming, Jean-Christophe Golaz, Vaishali Naik, and V. Ramaswamy. The roles of aerosol direct and indirect effects in past and future climate change. *J. Geophys. Res. Atmos.*, 118(10):4521–4532, 2013. ISSN 2169-8996.

Sergey Malyshev, Elena Shevliakova, Ronald J Stouffer, and Stephen W Pacala. Contrasting local versus regional effects of Land-Use-Change-Induced heterogeneity on historical climate: Analysis with the GFDL earth system model. *J. Clim.*, 28(13):5448–5469, 2015.

R.-S. Massad, E. Nemitz, and M. A. Sutton. Review and parameterisation of bi-directional ammonia exchange between vegetation and the atmosphere. *Atmos. Chem. Phys.*, 10(21):10359–10386, 2010.

P. C. D. Milly, Sergey L. Malyshev, Elena Shevliakova, Krista A. Dunne, Kirsten L. Findell, Tom Gleeson, Zhi Liang, Peter Phillipps, Ronald J. Stouffer, and Sean Swenson. An enhanced model of land water and energy for global hydrologic and earth-system studies. *J. Hydrometeorol.*, 15(5):1739–1761, June 2014. ISSN 1525-755X.

Vaishali Naik, Larry W. Horowitz, Arlene M. Fiore, Paul Ginoux, Jingqiu Mao, Adetutu M. Aghedo, and Hiram Levy. Impact of preindustrial to present-day changes in short-lived pollutant emissions on atmospheric composition and climate forcing. *J. Geophys. Res. Atmos.*, 118(14):8086–8110, July 2013. ISSN 2169-8996.

Eiko Nemitz, Celia Milford, and Mark A. Sutton. A two-layer canopy compensation point model for describing bi-directional biosphere-atmosphere exchange of ammonia. *Quart. J. Roy. Meteor. Soc.*, 127(573):815–833, April 2001. ISSN 1477-870X.

Tran B. Nguyen, John D. Crounse, Alex P. Teng, Jason M. St Clair, Fabien Paulot, Glenn M. Wolfe, and Paul O. Wennberg. Rapid deposition of oxidized biogenic compounds to a temperate forest. *Proc. Natl. Acad. Sci. U.S.A.*, 112(5):E392–E401, February 2015. ISSN 0027-8424, 1091-6490. doi: 10.1073/pnas.1418702112. URL `http://www.pnas.org/content/112/5/E392`.

Raùl Ochoa-Hueso, Edith B. Allen, Cristina Branquinho, Cristina Cruz, Teresa Dias, Mark E. Fen, Esteban Manrique, M. Esther Pérez-Corona, Lucy J. Sheppard, and William D. Stock. Nitrogen deposition effects on mediterranean-type ecosystems: An ecological assessment. *Environ. Pollut.*, 159(10):2265 – 2279, 2011. ISSN 0269-7491.

J. Padro, H. H. Neumann, and G. Den Hartog. Dry deposition velocity estimates of SO_2 from models and measurements over a deciduous forest in winter. *Water Air Soil Pollut.*, 68(3-4):325–339, June 1993. ISSN 0049-6979, 1573-2932.

F. Paulot, D. J. Jacob, R. W. Pinder, J. O. Bash, K. Travis, and D. K. Henze. Ammonia emissions in the United States, European Union, and China derived by high-resolution inversion of ammonium wet deposition data: Interpretation with a new agricultural emissions inventory (MASAGE_NH3). *J. Geophys. Res. Atmos.*, 119(7): 4343–4364, April 2014. ISSN 2169-8996.

F. Paulot, P. Ginoux, W. F. Cooke, L. J. Donner, S. Fan, M.-Y. Lin, J. Mao, V. Naik, and L. W. Horowitz. Sensitivity of nitrate aerosols to ammonia emissions and to nitrate chemistry: implications for present and future nitrate optical depth. *Atmos. Chem. Phys.*, 16(3):1459–1477, 2016. doi: 10.5194/acp-16-1459-2016. URL `http://www.atmos-chem-phys.net/16/1459/2016/`.

A. Petroff and L. Zhang. Development and validation of a size-resolved particle dry deposition scheme for application in aerosol transport models. *Geosci. Model Dev.*, 3(2):753–769, December 2010. ISSN 1991-9603.

Gareth K. Phoenix, Bridget A. Emmett, Andrea J. Britton, Simon J. M. Caporn, Nancy B. Dise, Rachel Helliwell, Laurence Jones, Jonathan R. Leake, Ian D. Leith, Lucy J. Sheppard, Alwyn Sowerby, Michael G. Pilkington, Edwin C. Rowe, Mike R. Ashmore, and Sally A. Power. Impacts of atmospheric nitrogen deposition: responses of multiple plant and soil parameters across contrasting ecosystems in long-term field experiments. *Glob. Chang. Biol.*, 18(4):1197–1215, April 2012. ISSN 1365-2486.

A. G. Ponette-González, K. C. Weathers, and L. M. Curran. Tropical land-cover change alters biogeochemical inputs to ecosystems in a Mexican montane landscape. *Ecol. Appl.*, 20(7):1820–1837, January 2010. ISSN 1939-5582.

Felix T. Portmann, Stefan Siebert, and Petra Döll. Mirca2000 — global monthly irrigated and rainfed crop areas around the year 2000: A new high-resolution data set for agricultural and hydrological modeling. *Global Biogeochem. Cycles*, 24(1):GB1011, 03 2010.

Keywan Riahi, Shilpa Rao, Volker Krey, Cheolhung Cho, Vadim Chirkov, Guenther Fischer, Georg Kindermann, Nebojsa Nakicenovic, and Peter Rafaj. Rcp 8.5—a scenario of comparatively high greenhouse gas emissions. *Clim. Chang.*, 109(1-2):33–57, 2011.

Stuart Riddick, Daniel Ward, Peter Hess, Natalie Mahowald, Raia Massad, and Elisabeth Holland. Estimate of changes in agricultural terrestrial nitrogen pathways and ammonia emissions from 1850 to present in the community earth system model. *Biogeosciences*, 13(11):3397–3426, jun 2016. doi: 10.5194/bg-13-3397-2016. URL `https://doi.org/10.5194/bg-13-3397-2016`.

Michele M. Rienecker, Max J. Suarez, Ronald Gelaro, Ricardo Todling, Julio Bacmeister, Emily Liu, Michael G. Bosilovich, Siegfried D. Schubert, Lawrence Takacs, Gi-Kong Kim, Stephen Bloom, Junye Chen, Douglas Collins, Austin Conaty, Arlindo da Silva, Wei Gu, Joanna Joiner, Randal D. Koster, Robert Lucchesi, Andrea Molod, Tommy Owens, Steven Pawson, Philip Pegion, Christopher R. Redder, Rolf Reichle, Franklin R. Robertson, Albert G. Ruddick, Meta Sienkiewicz, and Jack Woollen. MERRA: NASA's Modern-Era Retrospective Analysis for Research and Applications. *J. Clim.*, 24(14):3624–3648, July 2011. ISSN 0894-8755.

Donna B. Schwede and Gary G. Lear. A novel hybrid approach for estimating total deposition in the United States. *Atmos. Environ.*, 92:207–220, August 2014. ISSN 1352-2310.

Elena Shevliakova, Stephen W. Pacala, Sergey Malyshev, George C. Hurtt, P. C. D. Milly, John P. Caspersen, Lori T. Sentman, Justin P. Fisk, Christian Wirth, and Cyril Crevoisier. Carbon cycling under 300 years of land use change: Importance of the secondary vegetation sink. *Global Biogeochem. Cycles*, 23(2):GB2022, 2009. ISSN 1944-9224.

Samuel M. Simkin, Edith B. Allen, William D. Bowman, Christopher M. Clark, Jayne Belnap, Matthew L. Brooks, Brian S. Cade, Scott L. Collins, Linda H. Geiser, Frank S. Gilliam, Sarah E. Jovan, Linda H. Pardo, Bethany K. Schulz, Carly J. Stevens, Katharine N. Suding, Heather L. Throop, and Donald M. Waller. Conditional vulnerability of plant diversity to atmospheric nitrogen deposition across the United States. *Proc. Natl. Acad. Sci. U.S.A.*, 113(15):4086–4091, April 2016. ISSN 0027-8424, 1091-6490. doi: 10.1073/pnas.1515241113. URL `http://www.pnas.org/content/113/15/4086`.

D Simpson, H Fagerli, J Jonson, S Tsyro, P Wind, and JP Tuovinen. The emep unified eulerian model. model description. emep msc-w report 12003. *The Norwegian Meteorological Institute, Oslo, Norway*, 2003.

R. Singles, M.A. Sutton, and K.J. Weston. A multi-layer model to describe the atmospheric transport and deposition of ammonia in great britain. *Atmospheric Environment*, 32(3):393–399, feb 1998. doi: 10.1016/s1352-2310(97)83467-x. URL `https://doi.org/10.1016/s1352-2310(97)83467-x`.

B. Smith, D. Wårlind, A. Arneth, T. Hickler, P. Leadley, J. Siltberg, and S. Zaehle. Implications of incorporating n cycling and n limitations on primary production in an individual-based dynamic vegetation model. *Biogeosciences*, 11(7):2027–2054, apr 2014. doi: 10.5194/bg-11-2027-2014. URL `https://doi.org/10.5194/bg-11-2027-2014`.

J. Storkey, A. J. Macdonald, P. R. Poulton, T. Scott, I. H. Köhler, H. Schnyder, K. W. T. Goulding, and M. J. Crawley. Grassland biodiversity bounces back from long-term nitrogen addition. *Nature*, 528(7582):401–404, December 2015. ISSN 0028-0836. doi: 10.1038/nature16444. URL `http://www.nature.com/nature/journal/v528/n7582/abs/nature16444.html`.

M.A. Sutton, E. Nemitz, J.W. Erisman, C. Beier, K. Butterbach Bahl, P. Cellier, W. de Vries, F. Cotrufo, U. Skiba, C. Di Marco, S. Jones, P. Laville, J.F. Soussana, B. Loubet, M. Twigg, D. Famulari, J. Whitehead, M.W. Gallagher, A. Neftel, C.R. Flechard, B. Herrmann, P.L. Calanca, J.K. Schjoerring, U. Daemmgen, L. Horvath, Y.S. Tang, B.A. Emmett, A. Tietema, J. Peñuelas, M. Kesik, N. Brueggemann, K. Pilegaard, T. Vesala, C.L. Campbell, J.E. Olesen, U. Dragosits, M.R. Theobald, P. Levy, D.C. Mobbs, R. Milne, N. Viovy, N. Vuichard, J.U. Smith, P. Smith, P. Bergamaschi, D. Fowler, and S. Reis. Challenges in quantifying biosphere–atmosphere exchange of nitrogen species. *Environmental Pollution*, 150(1):125–139, nov 2007. doi: 10.1016/j.envpol.2007.04.014. URL `https://doi.org/10.1016/j.envpol.2007.04.014`.

Mark A. Sutton, David Simpson, Peter E. Levy, Rognvald I. Smith, Stefan Reis, Marcel Van Oijen, and Wim De Vries. Uncertainties in the relationship between atmospheric nitrogen deposition and forest carbon sequestration. *Glob. Chang. Biol.*, 14(9):2057–2063, September 2008. ISSN 1365-2486.

Pamela H. Templer, Kathleen C. Weathers, Amanda Lindsey, Katherine Lenoir, and Lindsay Scott. Atmospheric inputs and nitrogen saturation status in and adjacent to Class I wilderness areas of the northeastern US. *Oecologia*, 177(1):5–15, November 2014. ISSN 0029-8549, 1432-1939.

Elise M. Tulloss and Mary L. Cadenasso. Nitrogen deposition across scales: hotspots and gradients in a california savanna landscape. *Ecosphere*, 6(9):art167, sep 2015. doi: 10.1890/es14-00440.1. URL `https://doi.org/10.1890/es14-00440.1`.

Massimo Vieno, Anthony J. Dore, Peter Wind, Chiara Di Marco, Eiko Nemitz, Gavin Phillips, Leonor Tarrasón, and Mark A. Sutton. Application of the EMEP unified model to the UK with a horizontal resolution of 5x 5 km2. In *Atmospheric Ammonia*, pages 367–372. Springer Netherlands, 2009. doi: 10.1007/978-1-4020-9121-6_21. URL https://doi.org/10.1007/978-1-4020-9121-6_21.

K. C. Weathers, G. M. Lovett, G. E. Likens, and R. Lathrop. The Effect of Landscape Features on Deposition to Hunter Mountain, Catskill Mountains, New York. *Ecol. Appl.*, 10(2):528–540, 2000. ISSN 1051-0761. doi: 10.2307/2641112. URL http://www.jstor.org/stable/2641112.

Kathleen C. Weathers, Samuel M. Simkin, Gary M. Lovett, and Steven E. Lindberg. Empirical Modeling of Atmospheric Deposition in Mountainous Landscapes. *Ecol. Appl.*, 16(4):1590–1607, August 2006. ISSN 1939-5582.

G. R. Wentworth, J. G. Murphy, K. B. Benedict, E. J. Bangs, and J. L. Collett Jr. The role of dew as a night-time reservoir and morning source for atmospheric ammonia. *Atmos. Chem. Phys.*, 16(11):7435–7449, June 2016. ISSN 1680-7324. doi: 10.5194/acp-16-7435-2016. URL http://www.atmos-chem-phys.net/16/7435/2016/.

Jason J. Williams, Serena H. Chung, Anne M. Johansen, Brian K. Lamb, Joseph K. Vaughan, and Marc Beutel. Evaluation of atmospheric nitrogen deposition model performance in the context of u.s. critical load assessments. *Atmospheric Environment*, 150:244–255, feb 2017. doi: 10.1016/j.atmosenv.2016.11.051. URL https://doi.org/10.1016/j.atmosenv.2016.11.051.

Wei Wu and Charles T. Driscoll. Impact of climate change on three-dimensional dynamic critical load functions. *Environ. Sci. Technol.*, 44(2):720–726, 2010. PMID: 20020745.

Zhiyong Wu, Donna B. Schwede, Robert Vet, John T. Walker, Mike Shaw, Ralf Staebler, and Leiming Zhang. Evaluation and intercomparison of five north american dry deposition algorithms at a mixed forest site. *Journal of Advances in Modeling Earth Systems*, jun 2018. doi: 10.1029/2017ms001231. URL https://doi.org/10.1029/2017ms001231.

S. Zaehle, A. D. Friend, P. Friedlingstein, F. Dentener, P. Peylin, and M. Schulz. Carbon and nitrogen cycle dynamics in the o-CN land surface model: 2. role of the nitrogen cycle in the historical terrestrial carbon balance. *Global Biogeochemical Cycles*, 24(1):n/a–n/a, feb 2010. doi: 10.1029/2009gb003522. URL https://doi.org/10.1029/2009gb003522.

Leiming Zhang, Michael D. Moran, Paul A. Makar, Jeffrey R. Brook, and Gong Sunling. Modelling gaseous dry deposition in aurams: a unified regional air-quality modelling system. *Atmos. Environ.*, 36:537—560, 2002.

L. Zhu, D. Henze, J. Bash, G.-R. Jeong, K. Cady-Pereira, M. Shephard, M. Luo, F. Paulot, and S. Capps. Global evaluation of ammonia bidirectional exchange and livestock diurnal variation schemes. *Atmos. Chem. Phys.*, 15(22):12823–12843, November 2015. ISSN 1680-7324. doi: 10.5194/acp-15-12823-2015. URL http://www.atmos-chem-phys.net/15/12823/2015/.

Manuscript prepared for Atmos. Chem. Phys.
with version 2014/09/16 7.15 Copernicus papers of the LaTeX class copernicus.cls.
Date: 9 November 2018

Representing sub-grid scale variations in nitrogen deposition associated with land use in a global Earth System Model: implications for present and future nitrogen deposition fluxes over North America

Fabien Paulot[1,2], Sergey Malyshev[1], Tran Nguyen[3], John D. Crounse[4], Elena Shevliakova[1], and Larry W. Horowitz[1]

[1]Geophysical Fluid Dynamics Laboratory, National Oceanic and Atmospheric Administration, Princeton, New Jersey, USA
[2]Program in Atmospheric and Oceanic Sciences, Princeton University, New Jersey, USA
[3]Department of Environmental Toxicology, UC Davis, Davis, California, USA
[4]Division of Geological and Planetary Sciences, Caltech, Pasadena, California, USA

Correspondence to: Fabien.Paulot@noaa.gov

Abstract. Reactive nitrogen (N) emissions have increased over the last 150 years as a result of greater fossil fuel combustion and food production. The resulting increase in N deposition can alter the function of ecosystems, but characterizing its ecological impacts remains challenging, in part because of uncertainties in model-based estimates of N dry deposition. Here, we ~~leverage the tiled structure of the land component (LM3) of the~~ use the Geophysical Fluid Dynamics Laboratory (GFDL) ~~Earth System Model to~~ atmospheric chemistry-climate model (AM3) coupled with the GFDL land model (LM3) to estimate dry deposition velocities. We leverage the tiled structure of LM3 to represent the impact of physical, hydrological, and ecological heterogeneities on the surface removal of chemical tracers. We show that this framework can be used to estimate N deposition at more ecologically-relevant scales (e.g., natural vegetation, water bodies) than from the coarse-resolution global ~~chemistry–climate model (GFDL-AM3)~~model AM3. Focusing on North America, we show that the faster removal of N over forested ecosystems relative to cropland and pasture implies that ~~coarse resolution~~ coarse-resolution estimates of N deposition from global models systematically underestimate N deposition to natural vegetation by 10 to 30% in the Central and Eastern US. Neglecting the ~~subgrid~~ sub-grid scale heterogeneity of dry deposition velocities also results in an underestimate (overestimate) of the amount of reduced (oxidized) nitrogen deposited to water bodies. Overall, changes in land cover associated with human activities are found to slow down the removal of N from the atmosphere, causing a reduction in the dry oxidized, dry reduced, and total (wet+dry) N deposition over the contiguous US of 8%, 26%, and 6%, respectively. We also find that the reduction in the overall rate of removal of N associated with land-use change tends to increase

N deposition on the remaining natural vegetation and facilitate N export to Canada. We show that ~~subgrid~~ sub-grid scale differences in the surface removal of oxidized and reduced nitrogen imply that projected near-term (2010–2050) changes in oxidized (-47%) and reduced (+40%) US N emissions will cause opposite changes in N deposition to water bodies (increase) and natural vegetation (decrease) in the Eastern US, with potential implications for acidification and ecosystems.

1 Introduction

Fossil fuel combustion and food production release reactive nitrogen (N) to the atmosphere (Fowler et al., 2013). Once in the atmosphere, N can be transported over long distances before it is removed by dry and wet deposition, providing greater N inputs to otherwise pristine regions (e.g., national parks, boreal forests) (Paulot et al., 2014; Malm et al., 2016). Since N can be a limiting nutrient, the increase in N deposition may promote ecosystem productivity, (Townsend et al., 1996; Magnani et al., 2007; Pregitzer et al., 2008; Reay et al., 2008; Dezi et al., 2010; Wårlind et al., 2014; Devaraju et al., 2015) especially in boreal regions (Högberg, 2012; Gundale et al., 2014; Fleischer et al., 2015). Increasing N deposition can also cause adverse environmental impacts for terrestrial ecosystems including soil acidification, loss of biodiversity, and eutrophication (Stevens et al., 2004; Bobbink et al., 2010; Sutton et al., 2011; Pardo et al., 2011; Sheppard et al., 2011; Phoenix et al., 2012; Erisman et al., 2013; de Vries et al., 2015; Simkin et al., 2016). In the US, oxidized N deposition is projected to decrease as a result of effective controls on NO emissions, but deposition of reduced N ($NH_x \equiv NH_3 + NH_4^+$), primarily from agricultural emissions of NH_3, is projected to remain elevated or even increase (Dentener et al., 2006; Ellis et al., 2013; Paulot et al., 2013; Lamarque et al., 2013; Li et al., 2016). This raises concerns of irreversible damages to sensitive biomes (Pardo et al., 2011; Meunier et al., 2016; Grizzetti, 2011; Dise, 2011), such as high-elevation lakes (Wolfe et al., 2003; Baron et al., 2012; Lepori and Keck, 2012), and organisms (e.g., lichen (Johansson et al., 2012)).

Significant challenges remain in quantifying the long-term impacts of N deposition on ecosystems in a changing climate (Sutton et al., 2008; Wu and Driscoll, 2010; Phoenix et al., 2012; Högberg, 2012; de Vries et al., 2015; Storkey et al., 2015), including uncertainties in the speciation, magnitude and spatial distribution of the N deposition flux itself ~~(Sutton et al., 2008; Ochoa-Hueso et al., 2011; Fleischer et al., 2013). N is removed from the atmosphere by wet (i.e., precipitation) and dry (i.e., surface) deposition (Dentener et al., 2006). Much progress has been achieved in characterizing present-day N depositionby using~~ (Sutton et al., 2008; Ochoa-Hueso et al., 2011; Jickells et al., 2013; Fleischer et al., 2013). Many approaches have been developed to provide high-resolution, ecosystem-relevant estimates of both wet and dry N deposition, including statistical models (Singles et al., 1998; Dore et al., 2007; Weathers et al., 2006; Dore et al., 2012 high-resolution nested chemical transport model ~~combined~~ ($\simeq 4 \times 4 km$ (Vieno et al., 2009; Simkin et al., 2016)), and hybrid approaches that combine high-resolution regional chemical transport models with observed N fluxes and atmospheric concentrations (e.g. using the Community Multiscale Air Qual-

ity Modeling System (Schwede and Lear, 2014; Bytnerowicz et al., 2015; Williams et al., 2017)). However, the ~~requirement for observations and the~~ elevated computational requirement associated with high-resolution atmospheric models ~~limit the applicability of such approach to a few regions (Western Europe and the North America) over limited time periods (mostly post 2000). In particular,~~ ~~assessments of the~~ make such approaches impractical for assessing the long-term impact of N deposition on ecosystems, its sensitivity to climate change, and ultimately its coupling with the carbon cycle (Smith et al., 2014; Zaehle et al., 2010; Fleischer et al., 2013; Dirnböck et al., 2017; Fleischer et al., 2015)~~require estimates of historical and future N deposition~~ . For such questions, estimates of N deposition are generally derived from global ~~chemistry-climate models (e.g, Dentener et al. (2006); Lamarque et al. (2013)). However, the~~ models with coarse resolution ($\simeq$ 100km~~) of such models may introduce significant biases in N dry deposition fluxes~~, (Dentener et al., 2006; Lamarque et al., 2013)). This introduces a large uncertainty (Hertel, 2011) in N deposition estimates especially for dry deposition, which can vary over short distances ($\sim$1 km) in response to changes in the physical, hydrological, and ecological state of the surface (Weathers et al., 2000; Hicks, 2006, 2008; De Schrijver et al., 2008; Ponette-González et al., 2010; Te

The goal of this study is to develop a framework to diagnose ecosystem-specific N dry deposition fluxes within a global chemistry climate model on decadal to ~~centenial~~ centennial time scales. First we describe the coupling of the Geophysical Fluid Dynamics Laboratory (GFDL) land-model (LM3) to the GFDL atmospheric chemistry–climate model (AM3) to represent the impact of natural (e.g., vegetation type, soil and canopy wetness) and man-made (e.g., deforestation, cropping) heterogeneities on dry deposition. We then show that the tiled structure of LM3 can be leveraged to derive N deposition on a more ecologically-relevant scale (e.g., deposition on water bodies or natural vegetation). Finally, we discuss how this framework can be used to better represent the impact of land-use change and future trends in N emissions on N deposition.

2 Methods

2.1 Model description

We use an updated version of the GFDL AM3 atmospheric chemistry–climate model (Donner et al., 2011; Naik et al., 2013; Paulot et al., 2016) to simulate atmospheric dynamics and chemistry. Except for the treatment of dry deposition, the model configuration is identical to the one recently described by Paulot et al. (2016) and Paulot et al. (2017), including updates to wet deposition and the chemistry of sulfate and nitrate. The horizontal resolution of the model is 200km with 48 vertical levels.

In ~~previous versions of~~ AM3, the surface removal of chemical tracers ~~was~~ is calculated using a prescribed monthly climatology of dry deposition velocities (Naik et al., 2013; Paulot et al., 2016). The lack of a dynamic representation of dry deposition reduces the ability of the model to capture the impact of past and future variability in environmental conditions (e.g., drought (Wu et al., 2016), climate change) and land-use change on atmospheric chemistry. We note that these limitations are

not specific to AM3 but affect all chemical transport models that do not include a comprehensive land model (Ellis et al., 2013; Ran et al., 2017).

Here, we ~~use the GFDL land model(~~describe the development of a new model, in which dry deposition of gaseous and aerosol species is calculated within the dynamic vegetation model LM3 ~~) (Shevliakova et al., 2009; Milly et al., 2014)to represent the impact of surface properties on dry deposition.~~ (Shevliakova et al., 2009; Milly et al., 2014). The combined model will be referred to as AM3-LM3-DD hereafter.

LM3 is a comprehensive climate ~~land-model~~ land model that includes detailed representations of vegetation dynamics and hydrology and is designed to be run over decadal to century time scales under both historical and future conditions. ~~The combined model will be referred to as AM3-LM3-DD hereafter.~~

LM3 can be run both coupled with AM3 and in standalone mode with prescribed meteorological fields (Milly et al., 2014).

In LM3, ~~land use~~ the heterogeneity of the land surface and vegetation is represented using a sub-grid mosaic of tiles ~~. Each tile represents a different land type including water bodies, glacier, and four kinds of~~ (Shevliakova et al., 2009; Malyshev et al., 2015) as illustrated in Fig. 1. Each tile has distinct energy and moisture balances for a vegetation–snow–soil column, biophysical properties, and exchanges of radiant and turbulent fluxes with the overlying atmosphere. LM3 predicts physical, biogeochemical, and ecological characteristics for each sub-grid land surface tile from the top of the vegetation canopy to the bottom of the soil column, including leaves and canopy temperature, canopy-air specific humidity, stomatal conductance, snow cover and depth, runoff, vertical distribution of soil moisture, ice, and temperature. The land-use ~~types: cropland, pasture, secondary vegetation, i. e. vegetation in a state of recovery after logging or abandonment of pasture and cropland, and undisturbed vegetation, hereafter referred to as natural vegetation (Shevliakova et al., 2009; Malyshev et al., 2015). The spatial distribution and spatial extent of water bodies and glaciers are time–invariant. The transition rates among vegetated tiles are based on the Coupled Model Intercomparison Project, phase 5 (CMIP5) historical reconstructions of land-use up to 2005 and projections from integrated assessment models for 2005~~ history is prescribed from the Hurtt et al. (2011) reconstruction for each grid cell in terms of annual transition rates among four distinct land-use types: undisturbed (hereafter referred to as natural), crops, pastures, and secondary vegetation. Secondary vegetation is defined in LM3 as the vegetation recovering after land-use and land-cover changes and not currently managed. This includes all abandoned agricultural land as well as the land where wood was harvested at least once in prior years. The model keeps track of different recovery states by creating a secondary vegetation tile every time a disturbance occurs and simulating the subsequent vegetation regrowth in the tile. To avoid unrestricted growth of the number of tiles, the number of secondary vegetation tiles is limited to ~~2100 (Hurtt et al., 2011). The history of land disturbances is represented by up to~~ 10 ~~secondary tiles~~ per grid cell in the configuration of LM3 used here. When more than 10 secondary

vegetation titles exist in a grid cell, secondary vegetation tiles with similar properties are merged (Shevliakova et al., 2009), while preserving water, energy, and carbon balances. ~~Each land tile has distinct physical, hydrological, and ecological properties (Milly et al., 2014).~~ Land properties that affect the surface removal of chemical tracers, such as snow cover, canopy ~~wetness~~liquid water and snow mass, surface and canopy temperature, leaf area index (LAI), stomatal conductance, and vegetation height are all prognostic ~~(Malyshev et al., 2015).~~ (Shevliakova et al., 2009). Vegetation carbon is partitioned into five pools: leaves, fine roots, sapwood, heartwood, and labile storage. The model simulates changes in vegetation and soil carbon pools, as well as the carbon exchange among these pools and the atmosphere. The sizes of the pools are modified daily depending on the carbon uptake according to a set of allocation rules. Additionally, the model simulates changes in the vegetation carbon pools due to phenological processes, natural mortality, and fire. LAI is determined by vegetation leaf biomass and specific leaf area, prescribed for each vegetation type. Each vegetated tile has a unique vegetation type (C3 grass, C4 grass, temperate deciduous, coniferous, or tropical vegetation), which is determined based on biogeographical rules that take into account environmental conditions as well as ~~management for pasture (grazing) and cropland (planting and harvesting) .~~ the current state of the vegetation in each tile (Shevliakova et al., 2009). The fraction of the canopy covered by liquid water (f_l) and snow (f_s) are estimated from the intercepted canopy liquid water mass (w_l) and snow mass (w_s) following Bonan (1996):

$$f_i = \left(\frac{w_i}{W_{i,max}}\right)^{\frac{2}{3}} \qquad i \in \{l, s\} \tag{1}$$

where $W_{l,max} = 0.02 kg m^{-2}$ and $W_{s,max} = 0.2 kg m^{-2}$ are the maximum liquid water and snow holding capacities, respectively. If both snow and liquid water are present simultaneously, water and snow are assumed to be distributed independently of each other.

The representation of management practices is important in determining the impact of land-use change on dry deposition, as it affects the vegetation type, and the seasonality of the vegetation cover. In LM3, crop harvesting and pasture grazing are performed annually at the end of the calendar year (Malyshev et al., 2015). Previous work has shown that this treatment contributes to an underestimate of the impact of management on land cover (Malyshev et al., 2015)~~and~~ . To address these biases, we make the following ~~revisions~~modifications. For pasture, we assume that 25% of leaf biomass ~~is~~ removed daily by grazing, provided LAI exceeds 2 to avoid overgrazing. This higher grazing frequency ~~prevents the growth of trees~~ and intensity prevent the excessive growth of vegetation biomass on pasture in the tropics and mid latitudes~~on pasture~~, a problem which was noted in previous versions of LM3 (Malyshev et al., 2015) ~~. For crops,~~ leading to misclassification of pasture vegetation cover as forests (Malyshev et al., 2015). LM3 does not estimate the cropping schedule (e.g., Bondeau et al. (2007)), so we specify planting and harvesting dates from the global monthly irrigated and rainfed crop areas climatology (Portmann et al., 2010). The impact of management

practices on the timing and magnitude of agricultural emissions (e.g., Paulot et al. (2014)) is not accounted for in AM3-LM3-DD.

The tiled structure of LM3 is especially useful to diagnose fluxes to areas, such as natural ~~vegetations~~ vegetation or water bodies, which are generally not well-represented by the average properties of the grid-box, in which they are located, because of their small geographical extent (Fig. S1).

The dry deposition velocity ($v_d(X)$) for ~~a compound~~ species X is calculated independently for each tile following the widely used electrical circuit analogy (Fig. 1) (Hicks et al., 1987; Wesely, 1989; Zhang et al., 2001, 2003).

$$v_d(X) = \left[R_a + \frac{1}{\frac{1}{R_{ac,g} + R_{b,g}(X) + R_{sf,g}(X)} + \frac{1}{R_{ac,v} + \frac{1}{[R_{b,s}+R_{sf,s}]^{-1} + \frac{1}{R_{b,v}+\left[R_{sf,v}^{-1}+(R_m+R_s)^{-1}\right]^{-1}}}}} \right]^{-1} \quad (2)$$

Briefly, the aerodynamic resistance (R_a) to the exchange of tracers between the canopy and the atmosphere is determined using Monin-Obukhov similarity theory. The aerodynamic conductance to the ground ($R_{ac,g}$) and to the vegetation ($R_{ac,v}$) are independent of the chemical tracer and taken from Erisman (1994) and ~~Bonan (1996)~~Choudhury and Monteith (1988), respectively.

$$R_{ac,g} = \frac{u_\star}{14(LAI+SAI)h} \quad (3)$$

$$R_{ac,v} = (LAI+SAI)\cdot g_b \text{ with } g_b = 0.01(1-exp(-3/2)/3)\sqrt{\mathrm{V}} \quad (4)$$

where SAI, h, and V are the stem area index, the height of the vegetation, and the normalized wind at the top of the canopy, respectively.

We focus next on the representation of the dry deposition of gases, which is much faster than that of fine particles (Zhang et al., 2002).

Following Jensen and Hummelshøj (1995) and Jensen and Hummelshøj (1997), the canopy laminar resistance ($R_{b,v}$) is defined as:

$$R_{b,v}(X) = \frac{1}{D_X}\left(\frac{u_\star}{\nu} LAI\right)^{-2/3} (100lw)^{1/3} \quad (5)$$

where $u_\star$ is the friction velocity, lw the ~~leaf width~~ characteristic obstacle length of the canopy (Table S1), ~~LAI the leaf area index,~~ ν the kinematic viscosity, and D_X the diffusivity of species X. Following Hicks et al. (1987), the stem laminar resistance is:

$$R_{b,s}(X) = \frac{2}{\kappa u_\star}\left(\frac{Sc(X)}{Pr}\right)^{2/3} \tag{6}$$

where Pr is the Prandtl number, $Sc(X)$ is the Schmidt number, the ratio of the kinematic to the mass diffusivity ($Sc \propto {D_X}^{-1}$), κ the von Karman constant ($\kappa = 0.4$). Similarly, the ground surface laminar resistance is:

$$R_{b,g}(X) = \frac{2}{\kappa u_{g\star}}\left(\frac{Sc(X)}{Pr}\right)^{2/3} \tag{7}$$

where $u_{g\star}$ is the friction velocity near the ground (Loubet et al., 2006). The stomatal resistance (~~$R_s X$~~ $R_s(X)$) is calculated as

$$R_s(X) = \sqrt{\frac{M(X)}{M(\mathrm{H_2O})}} R_s(\mathrm{H_2O}) \tag{8}$$

where $M(X)$ is the molecular weight of species X and $R_s(\mathrm{H_2O})$ is the stomatal resistance for water vapor, calculated according to the Ball-Berry-Leuning model (Leuning, 1995; Milly et al., 2014). This model accounts for the impact of water stress and CO_2 concentration, ~~two factors that are not included in many atmospheric chemistry models (Wesely, 1989; Wang et al., 1998; Emmons et al., 2010) but~~ which have been shown to modulate the response of surface ozone to drought (Huang et al., 2016) and CO_2 increase (Sanderson et al., 2007). Cuticle (v), stem (s), and ground (g) resistances for species X are parameterized based on SO_2 and O_3:

$$R_{sf,i}(X) = \frac{s(T)}{\gamma(X)}\left(\frac{\alpha(X)}{R_{sf,i}(\mathrm{SO_2})} + \frac{\beta(X)}{R_{sf,i}(\mathrm{O_3})}\right)^{-1} \qquad i \in \{\mathrm{v, s, g}\} \tag{9}$$

where $R_{sf,i}(\mathrm{SO_2})$ and $R_{sf,i}$(~~O3~~$\mathrm{O_3}$) are tabulated resistances (Table S1) for each surface type, and $\alpha(X)$ and $\beta(X)$ are weighting factors (Table S2) estimated using the solubility (for α) and reactivity (for β) of X (Wesely, 1989; Zhang et al., 2002), $s(T)$ is a temperature adjustment factor (Zhang et al., 2003), and $\gamma(X)$ is a codeposition adjustment, which reflects changes in $R_{sf,i}(\mathrm{X})$ associated with surface acidity (Erisman et al., 1994; Massad et al., 2010; Neirynck et al., 2011; Wu et al., 2016). Here, we use ~~a modified version of~~ the parameterizations of Massad et al. (2010) for NH_3 and Simpson et al. (2003) for SO_2:

$$\gamma(X) = \begin{cases} \exp(2 - r_{SN}) & X = \mathrm{SO_2} \text{ and } \alpha_{SN} \leq 2 \\ 6.35 r_{SN} & X = \mathrm{NH3} \\ 1 & \text{otherwise} \end{cases} \tag{10}$$

~~where $r_{SN} = 0.5\frac{2DEP(\mathrm{SO_2})+2DEP(\mathrm{SO4})+DEP(\mathrm{HNO3})+DEP(\mathrm{NO3})}{DEP(\mathrm{NH3})+DEP(\mathrm{NH4})}$ and $DEP(X)$ denotes the dry deposition of X integrated over the previous 24h.~~ To improve numerical stability, we estimate the

acid ratio (r_{SN}) using the ratio of the 24-hour integrated total dry deposition of acids to the dry deposition of ammonia and ammonium, rather than using the ratio of their surface concentrations (Massad et al., 2010; Simpson et al., 2003).

The bidirectional exchange of ammonia is not represented in AM3-LM3-DD (Massad et al., 2010; Flechard et al., 2013). This reflects in part uncertainties in the emission potential of vegetation and the lack of detailed treatment of agricultural activities in LM3 (Riddick et al., 2016). We thus expect AM3-LM3-DD to overestimate NH_3 dry deposition in source regions (Zhu et al., 2015; Sutton et al., 2007).

2.2 Experimental design

We perform two sets of global simulations representative of present-day (circa 2010) and future (2050) conditions. For present-day conditions, AM3-LM3-DD is run from 2007 to 2010 using 2007 as spin-up. The model is forced with observed sea surface temperatures and sea ice cover, and land use from the Representative Concentration Pathways 8.5 scenario (RCP8.5, Riahi et al. (2011)). Anthropogenic emissions are from the Hemispheric Transport of Air Pollution 2 (HTAPv2, Janssens-Maenhout et al. (2015)). Natural emissions are based on Naik et al. (2013), except for isoprene emissions, which are calculated interactively using the Model of Emissions of Gases and Aerosols from Nature (MEGAN, Guenther et al. (2006)). This simulation will be referred to as R2010 hereafter. An additional sensitivity experiment is performed (R2010_no_lu) with no anthropogenic land-use change, which is achieved by removing all vegetated tiles but the natural ones (expanding the area of the natural tiles). In both experiments, horizontal winds are nudged to those from the National Centers for Environmental Prediction reanalysis (Kalnay et al., 1996) to minimize meteorological variability between R2010 and R2010_no_lu.

For 2050, we use the vegetation, sea surface temperatures, and sea ice cover simulated by the GFDL-CM3 model under the RCP8.5 scenario in 2050 (Levy et al., 2013). RCP8.5 anthropogenic emissions for 2050 are used (Lamarque et al., 2011) except for NH_3, where we use the spatial distribution and seasonality of HTAPv2 emissions following Paulot et al. (2016). The model is run for 10 years with land-use fixed to year 2050 and we use the average of the last 9 years to minimize the impact of internal variability. This simulation will be referred to as R2050 hereafter. We perform two additional sensitivity experiments to characterize how land-use change (R2050_2010lu) and climate (R2050_2010climate) contribute to the change in deposition velocity between R2010 and R2050. The different model runs are summarized in Table 1.

3 Results and discussion

3.1 Evaluation of simulated v_d against observations

The resistance approach for calculating dry deposition velocities implemented in AM3-LM3-DD is similar to that used in most chemical transport models. However differences in implementations can result in large differences between simulated deposition velocities (Wu et al., 2018). To illustrate

Table 1. Model runs

Run ID	Climate	Land Use	Anthropogenic Emissions
R2010	2008–2010[a]	RCP8.5 (2008–2010)	HTAPv2
R2010_no_lu	2008–2010[a]	natural vegetation	HTAPv2
R2050	2050	RCP8.5 (2050)	RCP8.5 (2050)[b]
R2050_2010lu	2008–2010[a]	RCP8.5 (2008–2010)	RCP8.5 (2050)[b]
R2050_2010climate	2008–2010[a]	RCP8.5 (2050)	RCP8.5 (2050)[b]

[a] horizontal winds are nudged to NCEP

[b] with modified NH_3 emissions following Paulot et al. (2016)

these differences, Fig. 2 shows the sensitivity of $v_d(SO_2)$ and $v_d(NH_3)$ to temperature, wetness, and surface acidity in three global models: MOZART (Emmons et al., 2010), GEOS-Chem (Wang et al., 1998), and AM3-LM3–DD. Under dry conditions, GEOS-Chem and AM3-LM3–DD produce identical results for $v_d(SO_2)$, with the temperature dependence driven by that of the stomatal conductance. At low and high temperatures, $v_d(NH_3)$ is faster in AM3-LM3–DD than GEOS-Chem, which reflects small differences in the assumed surface pH (6.35 and 6.6 respectively). In contrast, MOZART assumes a surface pH=5 and accounts for changes in the effective solubility of SO_2 and NH_3 with temperature, similar to Nguyen et al. (2015). The increase in solubility with decreasing temperature results in faster $v_d(X)$ at cold temperature in MOZART, while the lower pH increases $v_d(NH_3)$ and decreases $v_d(SO_2)$. The impact of surface wetness on $v_d(X)$ is only considered in MOZART and AM3-LM3 DD. In MOZART the presence of dew more than doubles $v_d(SO_2)$ but reduces $v_d(NH_3)$ below 25°C. In contrast, both $v_d(NH_3)$ and $v_d(SO_2)$ increase in AM3-LM3–DD when the canopy is wet, which is supported by observations (Erisman et al., 1994, 1999; Massad et al., 2010). AM3-LM3–DD also accounts for the modulation of $R_{sf,v}(SO_2)$ and $R_{sf,v}(NH_3)$ by the acidity of the surface. Our results suggest that when $\alpha_{SN} = 2$, i.e. when the deposition of acids is twice as large as the deposition of bases, the impact of codeposition can be greater than that of canopy wetness. The large differences in the response of $v_d(SO_2)$ and $v_d(NH_3)$ to environmental conditions across three models highlight the need for ~~a more robust understanding of the mechanisms controlling $R_{sf,i}(X)$~~detailed evaluations of $v_d(X)$ across a wide range of conditions and chemical species (Wu et al., 2018).

3.2 ~~Experimental design~~

3.1.1 $v_d(SO_2)$

We ~~perform two sets of global simulations under~~ first evaluate the simulated present-day (~~2007–2010) and future (2050) conditions. For present-day conditions, AM3-LM3-DD is forced with observed sea surface temperature and sea ice cover. Horizontal winds are nudged to those from the National~~

~~Centers for Environmental Prediction reanalysis (Kalnay et al., 1996) to minimize meteorological variability across configurations. Anthropogenic emissions are from the Hemispheric Transport of Air Pollution 2 (HTAP 2, Janssens-Maenhout et al. (2015)). For 2050, we use the vegetation, sea surface temperature, and sea ice cover simulated by the GFDL-CM3 model under the Representative Concentration Pathways 8.5 scenario (Riahi et al., 2011) in 2050 (Levy et al., 2013). RCP8.5 anthropogenic emissions for 2050 are used (Lamarque et al., 2011) except for NH_3, where we use the spatial distribution and seasonality of HTAPv2 emissions (Janssens-Maenhout et al., 2015) following Paulot et al. (2016). The model is run for 10 years with land-use fixed to year 2050 and we use the average of~~ R2010) $v_d(SO_2)$ against a compilation of field-based $v_d(SO_2)$ observations (Table S3). We sample the simulated monthly diurnal cycle of $v_d(SO_2)$ at the location of the measurements in the ~~last 9 years to minimize the impact of internal variability.~~ tile that best represents the type of vegetation reported in the observations. We further distinguish between day-time (8am-5pm) and night-time (10pm-4am) samples and wet (wet fraction of the canopy greater than 10%) and dry periods.

4 ~~Results and discussion~~

3.1 ~~Evaluation~~

~~We first evaluate the representation of $v_d(SO_2)$ in AM3-LM3–DD for present-day (2007-2010) using observations collected over a wide range of surfaces.~~ Fig. 3 shows observed and simulated $v_d(SO_2)$ grouped among the four types of vegetation simulated by LM3 (deciduous, coniferous, tropical, and grass).

Simulated deposition velocities generally fall within a factor of 2 of the observations, with better agreement during the day than at night, when the model is biased high. ~~The model~~ This uncertainty range is similar to that reported by Wu et al. (2018) in different dry deposition models. More specifically, AM3-LM3-DD qualitatively captures the ~~winter to summer increase in $v_d(SO_2)$ over deciduous forestsas well as its increase with canopy wetness~~range of deposition velocities over forested ecosystems, including the slower deposition of SO_2 in winter than in summer and under dry than under wet conditions in deciduous forests, and the fast removal of SO_2 over coniferous forests. However, the model ~~underestimates~~ fails to capture the elevated $v_d(SO_2)$ ~~over grassland. Here, we do not account for the~~ (>1 cm/s) reported by several studies over grasslands. This may reflect uncertainties in the representation of ammonia emissions (e.g., no sub-grid ~~heterogeneity of anthropogenic NH_3 emissions , which would likely result in higher~~ heterogeneity), which could result in an underestimate of SO_2-NH_3 ~~concentrations and thus faster $v_d(SO_2)$ (Neirynck et al., 2011) over~~ co-deposition over crops or fertilized grasslands (Nemitz et al., 2001; Flechard et al., 2013).

~~There are fewer observations of the deposition velocity of individual N carriers in part because of measurement challenges (Nguyen et al., 2015).~~

3.0.1 v_d(HNO3, HCN, H_2O_2, OrgN)

Fig. 4 shows the observed ~~and simulated~~ deposition velocities for HNO_3, a range of organic nitrates (ISOPN, MVKN, PROPNN) derived from isoprene photooxidation (Paulot et al., 2009), ~~and HCNin summer over a mixed forest in the Southeast US. The simulated and observed deposition velocities of~~ HCN, and H_2O_2 ~~are also shown~~. We refer the reader to Nguyen et al. (2015) for information regarding the site and Caltech observations. We compare these observations with the simulated deposition velocities at this site decomposed into its stomatal, cuticle (wet and dry), stem, and ground components.

To facilitate the comparison between simulated and observed deposition velocities, we ~~run LM3 in standalone model using~~ use meteorological fields (wind speed, temperature, precipitation, and downward radiation) from the Modern-Era Retrospective Analysis for Research and Applications (MERRA) (Rienecker et al., 2011) to drive a standalone version of LM3-DD. This provides a more accurate representation of the site conditions than using meteorological fields simulated by AM3. ~~The measured compounds~~

The compounds measured by Nguyen et al. (2015) have different chemical properties, allowing us to evaluate the representation of different deposition pathways in AM3-LM3–DD. In particular, HNO_3 and H_2O_2 have negligible cuticular resistance ($R_{surf,v} \simeq 0$) (Nguyen et al., 2015), such that $v_d(X) \simeq [R_a + R_{b,v}(X)]^{-1}$ (ground deposition is negligible). ~~The model~~ Fig. 4 shows that LM3-DD captures both $v_d(H_2O_2)$ and $v_d(HNO_3)$ well, including the faster deposition of H_2O_2 relative to HNO_3, consistent with the dependence of R_b on $1/D_X \propto \sqrt{MW(X)}$ (equation 5). ~~v_d(H_2O_2) and v_d(HNO_3) are overestimated in the late afternoon and at night. This may reflect excessive mixing in the model during these time periods (i.e., R_a too low).~~ In contrast, the ~~deposition of HCN on cuticles is negligible~~ low solubility and low reactivity at the leaf surface of HCN produces a large non stomatal resistance ($R_{sf,v} \ggg 1$ s/m~~), so~~ , Nguyen et al. (2015)), such that $v_d(\mathrm{HCN}) \simeq R_s(\mathrm{HCN})^{-1}$. Comparison of observed and modeled v_d(HCN) suggests that the Ball-Berry-Leuning model captures the stomatal conductance well at this site. Since R_a, $R_{b,v}$, and R_s are well represented over the measurement period, we use observations of v_d(ISOPN), v_d(MVKN), and v_d(PROPNN) at this site to estimate α and β for these organic nitrates ~~.~~(Eq. 9). We find that ($\alpha = 7$, $\beta = 1$) provide a reasonable fit for all organic nitrates~~and~~ . These parameters imply that the deposition of isoprene-derived organic nitrates is primarily controlled by dry cuticles with small contributions of stomata and stems. We note that these parameters imply a much greater solubility and reactivity of organic nitrogen than in other models (e.g., $\alpha = 0$, $\beta = 0.5$ in AURAMS (Zhang et al., 2002)). While we use these ~~values globally~~parameters globally, such large differences warrant further investigations, as the deposition of organic nitrogen may account for over 25% of the overall N deposition but remains rarely measured (Jickells et al., 2013).

Finally, we note that the comparison against SOAS observations points to a significant high bias in simulated night-time deposition velocity. Since this bias is found for all species including H_2O_2 and

HNO_3, this suggests that the model underestimates the aerodynamic resistance (R_a) during these periods.

3.1 Impact of land heterogeneities on present-day N deposition

Fig. 5 shows the simulated dry deposition of oxidized N (dominated by HNO_3) and reduced N (dominated by NH_3) as well as the total N deposition (wet+dry) in North America. As noted in previous studies (Zhang et al., 2012; Lamarque et al., 2013), the overall pattern of N deposition mirrors the underlying distribution of NH_3 and NO emissions, with high deposition in the Northeast and greater contribution of reduced nitrogen to N deposition in the US Midwest ~~than~~ and North Carolina than elsewhere in the Eastern US.

The simulated dry deposition represents the sum of the deposition fluxes to the tiles that comprise each grid cell. Fig. 5 (middle column) shows that N deposition over natural vegetation is generally greater than the grid-cell average, which is consistent with faster deposition velocities over forests relative to grasslands ~~(Finkelstein, 2001; Hicks, 2006) (see supplementary materials).~~ (Finkelstein (2001); Hicks (2006) and Fig. S1). Overall, the simulated total N deposition to natural ecosystems exceeds the grid-box average deposition by 10 to 30% over most of the Eastern and Central US. This enhancement is largest in regions ~~that have experienced extensive deforestation~~ where land-use change has caused a large decrease in vegetation height and LAI (e.g., in the US ~~Northeast~~Midwest and Northeast, Fig. S2) and smallest in regions with little agricultural activity (e.g., most of Canada) or where managed vegetation differs little in height and LAI from natural vegetation (e.g., in the Western US, Fig. S2). Fig. 5 (middle column) also shows that the dry deposition of NH_x ~~is more sensitive to land-use change than that~~ exhibits a greater enhancement over natural vegetation than the dry deposition of NO_y, ~~which reflects the much faster deposition velocity of HNO_3 relative to NH_3~~ consistent with the greater sensitivity of $v_d(NH_3)$ than $v_d(HNO_3)$ to surface properties (Fig. ~~S2). Overall, the simulated total N deposition to natural ecosystems exceeds the grid-box average deposition by 10 to 30% over most of the Eastern and Central US~~S3). The enhancements of the dry deposition of NH_x over natural vegetation is likely to be underestimated in AM3-LM3-DD as the surface bidirectional exchange of NH_3 tends to reduce its deposition in source regions.

Fig. 5 (right column) also shows that water bodies receive more reduced N but less oxidized N through dry deposition than the grid-box average. These differences can be attributed to the large effective solubility of NH_3 in freshwater, which results in lower $R_{sf,g}(NH_3)$ than over vegetated surfaces ($R_{sf,g}(HNO_3)$ is low over all surfaces). ~~In contrast, our~~ Our model suggests that $v_d(HNO_3)$ is generally slower over water bodies than over vegetated surfaces because of the lower roughness height of water bodies (see Fig. ~~S2~~S3). The westward increase in the ratio of NH_3 to NO emissions thus results in water bodies receiving less N than the average grid cell in the Eastern US and Canada but more in the Central and Western US. .

~~In order to quantify the impact of land-use change on nitrogen deposition , we perform an additional simulation in which only natural vegetation is considered. Fig. 6 shows~~

3.2 Impact of anthropogenic land-use change on present-day N deposition

Fig. 6 shows the change in dry NO_y, dry NH_x, and total N deposition associated with anthropogenic land-use change, which is estimated by comparing R2010 and R2010_no_lu. We find that anthropogenic land-use change ~~has decreased~~ reduces dry NO_y, dry NH_x, and total N deposition over the contiguous US by 8%, 26%, and 6%, respectively. ~~This reflects the reduction in deposition velocity associated with lower LAI and height for crop and pasture relative to natural vegetation . This reduction of the overall deposition velocity near source regions~~ The reduction in N deposition associated with anthropogenic land-use change is largest in the Central and Eastern US, where deforestation has caused a large reduction in LAI and vegetation height (Fig. S2).

While anthropogenic land use is estimated to reduce the overall N deposition in the contiguous US, we find that it tends to increase the surface concentration of ~~N carrier~~reactive nitrogen species, which leads to greater N deposition on the remaining natural vegetation. ~~For instance,~~ Fig. 6 shows that land use has important implications for N deposition at national parks, which are best represented by natural vegetation tiles. For instance, we find that anthropogenic land-use change ~~has induced~~ is associated with a 14% ~~decrease of~~ reduction in the overall N deposition in the region of Shenandoah National Park, but an increase of 9% on natural vegetation in the same grid box. The slower removal of N near source regions also facilitates N export to remote regions, such as Eastern Canada, where N deposition (primarily through wet deposition) increases by more than 10%. This suggests that anthropogenic land-use change in North America has contributed to the increase of N deposition to natural ecosystems both near source regions and in remote receptor regions.

3.3 Implications for future N deposition

Fig. 7 shows the simulated ~~change in N deposition from 2010 to 2050 in response to changes in climate, anthropogenic emissions ,~~ difference between N deposition in 2008–2010 (R2010) and 2050 (R2050). This difference reflects changes in anthropogenic emissions as well as changes in climate and land properties induced by climate and land-use change~~in the RCP8.5 scenario (van Vuuren et al., 2011; Riahi et al., 2011). In this scenario, the fraction of land devoted to agriculture decreases in North America (Davies-Barnard et al., 2014), which results in a small increase of $v_d(HNO_3)$ and a larger increase of $v_d(NH_3)$ (Fig. S3). However, in our model the increase of $v_d(NH_3)$ is compensated by the decrease in acid deposition, which reduces $v_d(NH_3)$ especially in the Eastern US (see equation 10).~~

. Total N deposition is projected to increase by 9% over the contiguous US. Most of the increase is driven by greater deposition in the Midwest and Western US associated with higher NH_3 emissions (+40%). In contrast, N deposition is projected to decrease in the Eastern US following the decrease of NO emissions (-47%, mostly in the Eastern US). ~~These trends are~~

We find a small increase (<10%) in the deposition velocity of HNO_3 over most of the US between R2010 and R2050 (Fig. S4). This is attributed to a reduction in the land fraction devoted to agriculture in RCP8.5 between 2010 and 2050 (Davies-Barnard et al., 2014), which results in taller vegetation and higher LAI. The impact of this change in land use between 2010 and 2050 is larger for $v_d(NH_3)$, which increases by more >10% over most of the Midwest and Eastern US. However, in the Eastern and Midwest US, this increase is more than compensated by a reduction in acid deposition, which results in an overall decrease of $v_d(NH_3)$ of 10 to 20% over most of the Eastern US. This highlights the need to better characterize the impact of the co-deposition of acids and ammonia on the removal of ammonia to improve projection of future N deposition.

Fig. 7 also shows that trends in N deposition simulated for all land types tend to be amplified over natural vegetation~~consistent with~~ , because of the faster deposition velocities ~~. Water~~ as discussed earlier. In contrast, water bodies are projected to experience an increase in N deposition over most of the US, including in regions which experience an overall decrease in N deposition. This contrast is driven by the faster removal of NH_3 over water relative to managed vegetation, which result in greater sensitivity to changes in the emissions of reduced N. ~~These opposite responses~~ The different responses of N deposition on natural tiles and water tiles are important for projections of N deposition in national parks, where N deposition to both vegetation and water bodies is of concern. For instance, the changes in N deposition to natural vegetation from 2010 to 2050 at Voyageurs and Shenandoah national parks are 30% greater than simulated in the grid box where they are located, while N deposition to water bodies in the Shenandoah region is projected to increase by 16%, even though overall N deposition for the grid decreases by 18% in this region.

4 Conclusions

Our study highlights the importance of accounting for surface heterogeneities and anthropogenic land use in modulating the magnitude and trend of N deposition. Here, we leverage the tiled structure of the GFDL land model to efficiently represent the ~~subgrid~~ sub-grid scale heterogeneity of surface properties and their evolution in a changing climate. We have shown that the shift of N emissions from oxidized to reduced N in North America will exacerbate the sensitivity of N deposition to small-scale heterogeneities, which highlights the need to improve the representation of non-stomatal surface resistances ($R_{sf,v}$, $R_{sf,s}$, and $R_{sf,g}$) including their modulation by canopy wetness and acidity (Flechard et al., 2013; Wentworth et al., 2016; Wu et al., 2018).

Our approach is best suited to long time scales (decadal to centennial) and is complementary to ongoing efforts to improve the representation of present-day N deposition using a combination of high-resolution ~~model~~ models and observations (Schwede and Lear, 2014). Future work will aim at coupling the representation of dry deposition presented here to the N cycle in the GFDL land model (Gerber et al., 2010), which will enable us to represent the bidirectional exchange of NH_3

(Nemitz et al., 2001; Flechard et al., 2013; Bash et al., 2013) and improve our understanding of the impact of N deposition on ecosystems and carbon cycling (Magnani et al., 2007; Janssens et al., 2010; Fleischer et al., 2013, 2015).

Acknowledgement. This study was supported by NOAA Climate Program Office's Atmospheric Chemistry, Carbon Cycle, and Climate program. Caltech observations and JDC were supported by NSF (Grant #AGS-1240604). We thank V. Naik, A. Fiore, and J. Schnell for helpful comments.

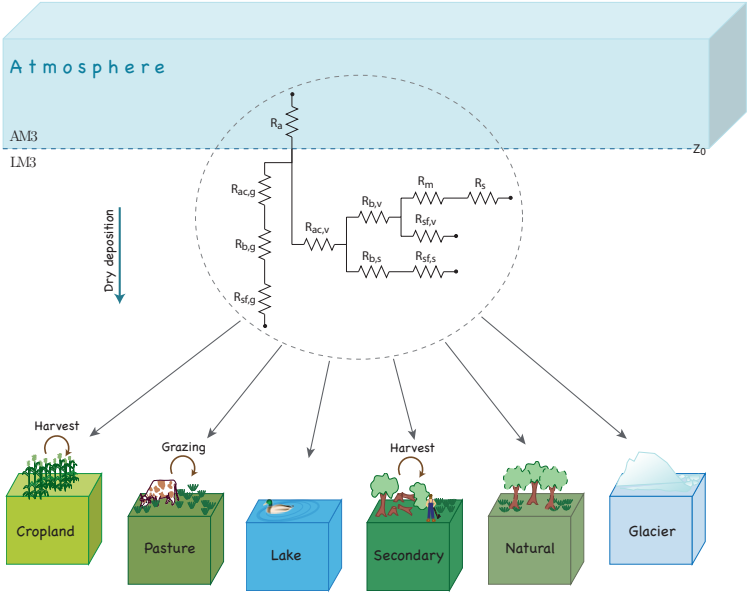

Figure 1. Schematic representation of the resistance scheme used to represent the dry deposition of gaseous tracers for each tile. R_a, $R_{b,i}$, R_{ac}, R_m , R_s, and $R_{sf,i}$ are the aerodynamic resistance, laminar resistance, canopy aerodynamic resistance, mesophyl resistance, stomatal resistance, and surface resistance, respectively. The g, s, and v indexes (i) refer to ground, stem, and vegetation. Note that for clarity deposition on soil and vegetation that are covered by snow or liquid water are not shown.

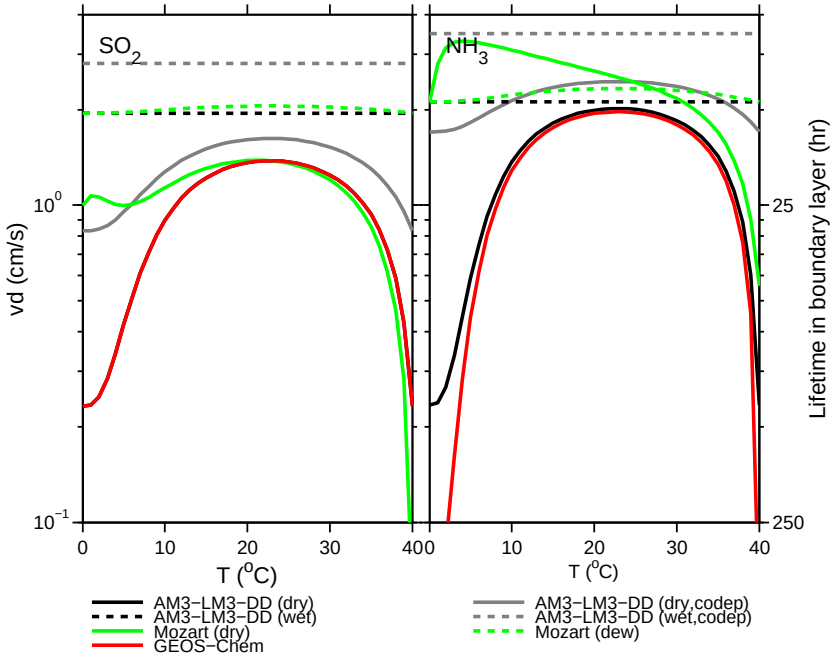

Figure 2. Simulated deposition velocity of NH_3 and SO_2 over a coniferous forest (LAI=5, $u_\star = 0.5$m/s, RH=80%) at different canopy wetness and temperature. To facilitate comparison across models, we use the same $R_a = 20$s/m, R_b (Hicks et al., 1987) and R_s (Wesely, 1989) for all models. Solar irradiation increases linearly from 0 to 800 W/m^2 with temperature. We neglect deposition to the ground and stems. Co-dep refers to the decrease in $R_{sf,v}(SO_2)$ and $R_{sf,v}(NH_3)$ associated with base and acid deposition respectively. For illustrative purposes, the ratio of acid to base deposition is set to 0.5 for SO_2 and 2 for NH_3. The lifetimes of SO_2 and NH_3 are estimated assuming a boundary layer height of 900m. GEOS-Chem and AM3-LM3–DD produce identical results for SO_2 under dry conditions.

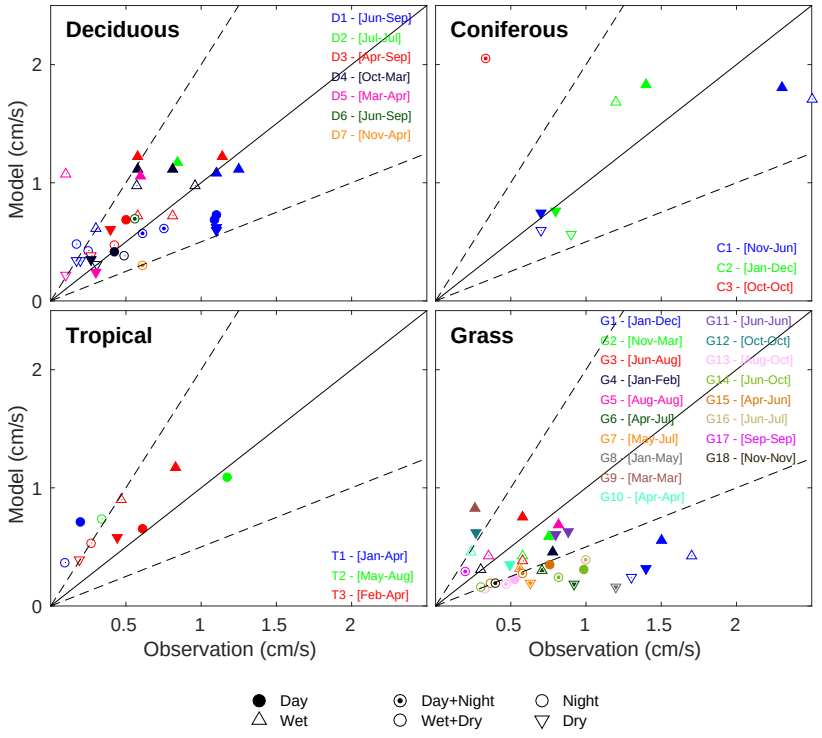

Figure 3. Observed and simulated deposition velocities of SO_2 for different vegetation types. The ~~model is sampled over the same vegetation type and months as the observations. The~~ symbol shape indicates the canopy status: wet (upward pointing triangle), dry (downward point triangle), circle (average). The symbol fill indicates the time period~~. For comparison with the models, wet conditions are defined as more than 10% of the canopy covered with dew or rain, daytime condition as 10am to 3pm local time, and nightime conditions as 10pm to 5am local time. Reference and time period for each observation are indicated for deciduous~~ : filled (~~D~~day), ~~coniferous~~ half-filled (~~C~~day+night), ~~tropical~~ empty (~~T~~night)~~, and grass~~. The monthly diurnal cycle of deposition velocities simulated by AM3-LM3-DD (~~G~~R2010 simulation) ~~(Finkelstein et al., 2000; Matt et al., 1987; Neirynck et al., 2011; Erisman, 1994; Granat and Richter, 1995; Matsuda et al., 2006; Feliciano et al., 2~~ sampled at each observation site in the tile that best represents the observed ecosystem accounting for the month, time of day and canopy wetness status when the observations were collected . References for the different sites are given in Table S3.

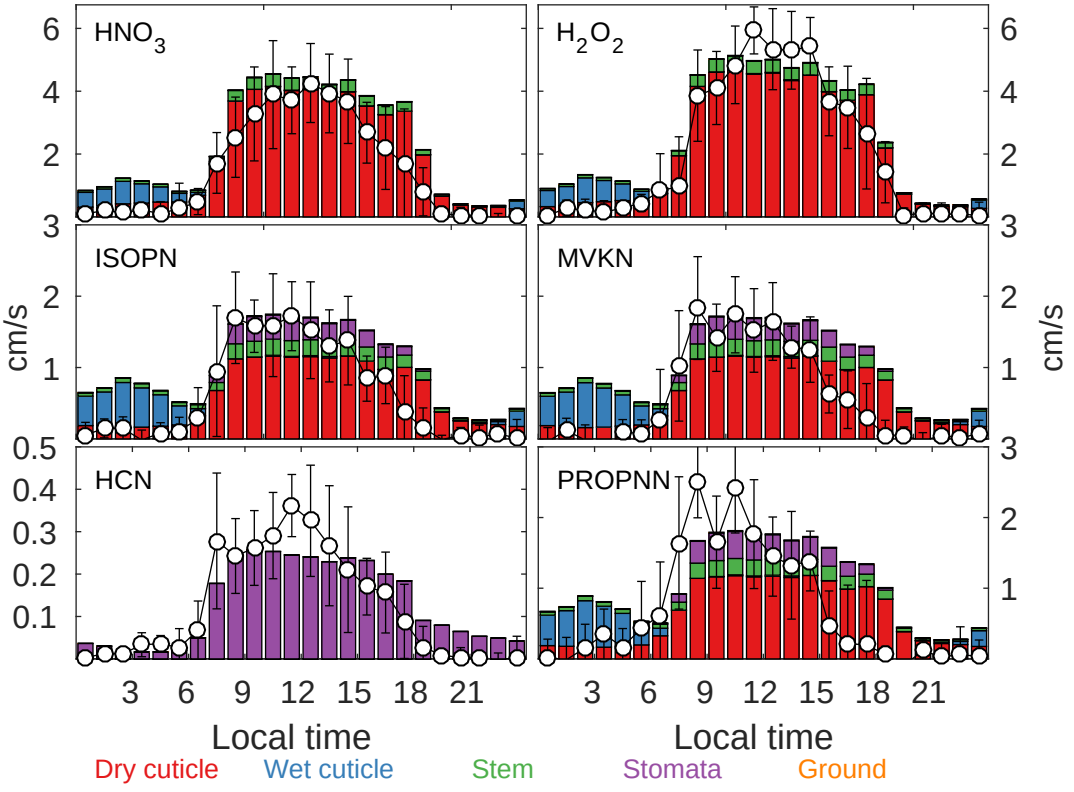

Figure 4. Observed (circles +/- standard deviation) and simulated (bars) dry deposition velocities for several nitrogen–containing species and hydrogen peroxide over the Talladega National Forest (Southeast US) in June 2013 (5 days, Nguyen et al. (2015)). The bar colors indicate the contribution of the different surfaces to the overall surface removal of the chemical tracer.

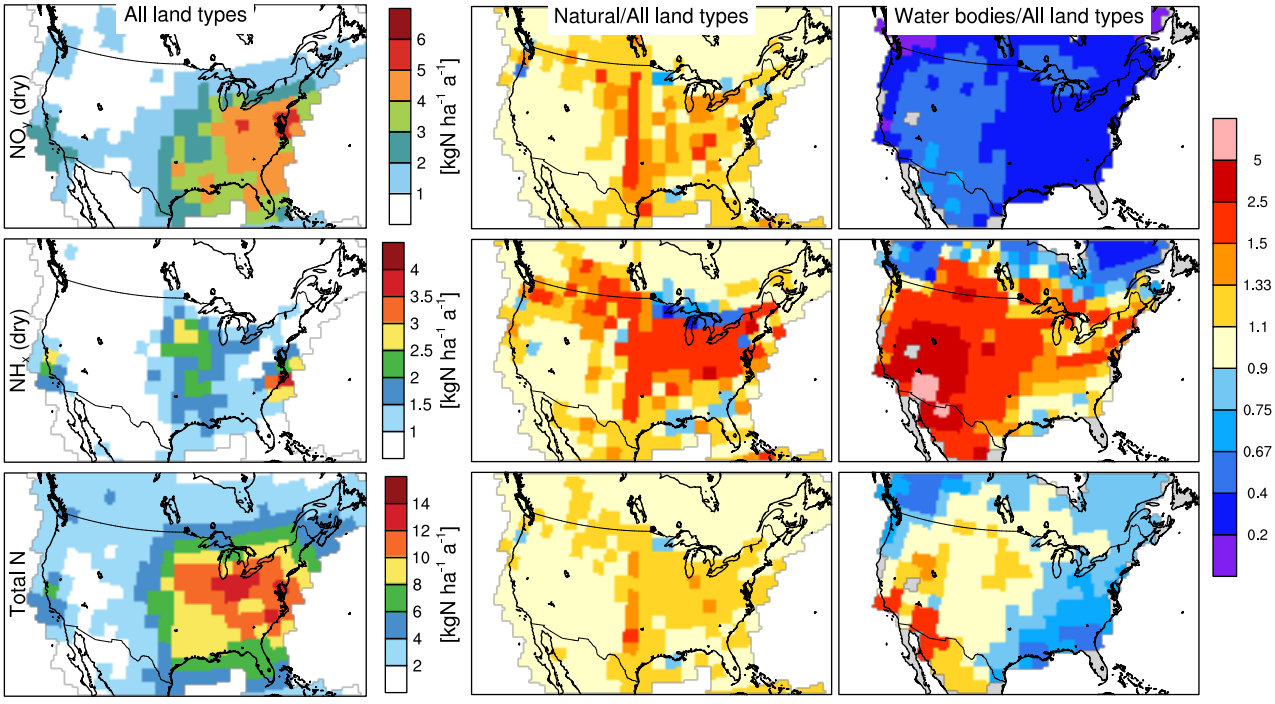

Figure 5. Simulated reactive nitrogen deposition (left column) from dry oxidized nitrogen deposition (first row), dry reduced nitrogen deposition (second row), and total nitrogen deposition (bottom row) over the 2008–2010 period. The ratio between the deposition on selected land types and the grid cell average deposition is shown in the middle (for natural vegetation) and right columns (water bodies)

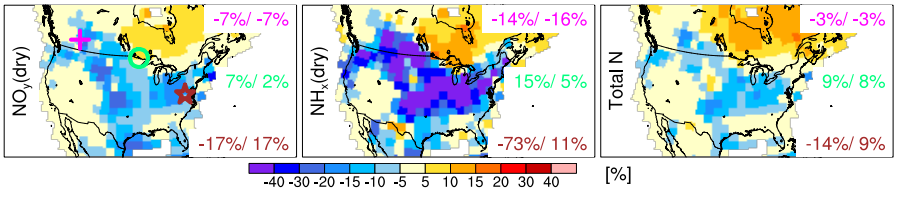

Figure 6. Relative change in the 2008–2010 average land deposition of dry oxidized nitrogen (left), dry reduced nitrogen (center), and total nitrogen (right) associated with anthropogenic land-use change. The relative change is shown as (with land-use - without land land-use)/with land-use. From top right to bottom right, the percentages indicate the change in N deposition at Banff National Park (cross), Voyageurs National Park (circle), and Shenandoah National Park (star) at the grid box level and on natural vegetation, a better proxy for these parks. ~~The fractional change in N deposition over the contiguous US is indicated in inset (bottom left).~~

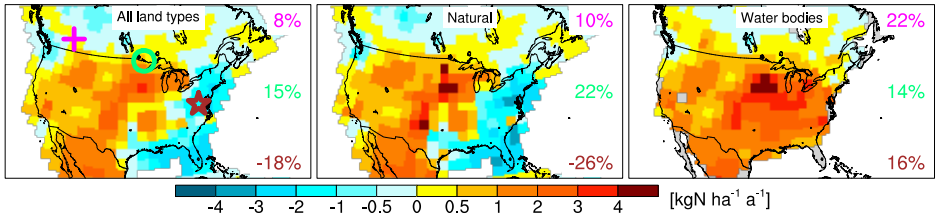

Figure 7. Simulated change in reactive nitrogen deposition from 2010 to 2050 in the RCP8.5 scenario at the grid box level (left), on natural tiles (center) and on water bodies (right). From top right to bottom right, the percentages indicate the change in N deposition at Banff National Park (cross), Voyageurs National Park (circle), and Shenandoah National Park (star) at the grid box level and on natural vegetation tiles respectively. The fractional change in N deposition over the contiguous US is indicated in inset (bottom left).

References

Baron, J. S., Hall, E. K., Nolan, B. T., Finlay, J. C., Bernhardt, E. S., Harrison, J. A., Chan, F., and Boyer, E. W.: The interactive effects of excess reactive nitrogen and climate change on aquatic ecosystems and water resources of the United States, Biogeochemistry, pp. 1–22, 2012.

Bash, J. O., Cooter, E. J., Dennis, R. L., Walker, J. T., and Pleim, J. E.: Evaluation of a regional air-quality model with bidirectional NH_3 exchange coupled to an agroecosystem model, Biogeosciences, 10, 1635–1645, 2013.

Bobbink, R., Hicks, K., Galloway, J., Spranger, T., Alkemade, R., Ashmore, M., Bustamante, M., Cinderby, S., Davidson, E., Dentener, F., Emmett, B., Erisman, J.-W., Fenn, M., Gilliam, F., Nordin, A., Pardo, L., and De Vries, W.: Global assessment of nitrogen deposition effects on terrestrial plant diversity: a synthesis, Ecol. Appl., 20, 30–59, 2010.

Bonan, G. B.: Land surface model (LSM version 1.0) for ecological, hydrological, and atmospheric studies: Technical description and users guide. Technical note, Tech. rep., National Center for Atmospheric Research, Boulder, CO (United States). Climate and Global Dynamics Div., 1996.

Bondeau, A., Smith, P., Zaehle, S., Schaphoff, S., Lucht, W., Cramer, W., Gerten, D., Lotze-Campen, H., Müller, C., Reichstein, M., et al.: Modelling the role of agriculture for the 20th century global terrestrial carbon balance, Global Change Biol., 13, 679–706, 2007.

Bytnerowicz, A., Johnson, R., Zhang, L., Jenerette, G., Fenn, M., Schilling, S., and Gonzalez-Fernandez, I.: An empirical inferential method of estimating nitrogen deposition to Mediterranean-type ecosystems: the San Bernardino Mountains case study, Environmental Pollution, 203, 69–88, doi:10.1016/j.envpol.2015.03.028, https://doi.org/10.1016/j.envpol.2015.03.028, 2015.

Choudhury, B. J. and Monteith, J. L.: A four-layer model for the heat budget of homogeneous land surfaces, Quarterly Journal of the Royal Meteorological Society, 114, 373–398, doi:10.1002/qj.49711448006, https://doi.org/10.1002/qj.49711448006, 1988.

Davies-Barnard, T., Valdes, P. J., Singarayer, J. S., Pacifico, F. M., and Jones, C. D.: Full effects of land use change in the representative concentration pathways, Environ. Res. Lett., 9, 114 014, doi:10.1088/1748-9326/9/11/114014, http://stacks.iop.org/1748-9326/9/i=11/a=114014, 2014.

De Schrijver, A., Staelens, J., Wuyts, K., Van Hoydonck, G., Janssen, N., Mertens, J., Gielis, L., Geudens, G., Augusto, L., and Verheyen, K.: Effect of vegetation type on throughfall deposition and seepage flux, Environ. Pollut., 153, 295–303, 2008.

de Vries, W., Hettelingh, J.-P., and Posch, M., eds.: Critical Loads and Dynamic Risk Assessments, vol. 25 of *Environmental Pollution*, Springer Netherlands, Dordrecht, 2015.

Dentener, F., Drevet, J., Lamarque, J. F., Bey, I., Eickhout, B., Fiore, A. M., Hauglustaine, D., Horowitz, L. W., Krol, M., Kulshrestha, U. C., Lawrence, M., Galy-Lacaux, C., Rast, S., Shindell, D., Stevenson, D., Van Noije, T., Atherton, C., Bell, N., Bergman, D., Butler, T., Cofala, J., Collins, B., Doherty, R., Ellingsen, K., Galloway, J., Gauss, M., Montanaro, V., Müller, J. F., Pitari, G., Rodriguez, J., Sanderson, M., Solmon, F., Strahan, S., Schultz, M., Sudo, K., Szopa, S., and Wild, O.: Nitrogen and sulfur deposition on regional and global scales: A multimodel evaluation, Global Biogeochem. Cycles, 20, B4003, 2006.

Devaraju, N., Bala, G., Caldeira, K., and Nemani, R.: A model based investigation of the relative importance of CO_2-fertilization, climate warming, nitrogen deposition and land use change on the global terrestrial carbon uptake in the historical period, Clim. Dyn., pp. 1–18, 2015.

Dezi, S., Medlyn, B. E., Tonon, G., and Magnani, F.: The effect of nitrogen deposition on forest carbon sequestration: a model-based analysis, Glob. Chang. Biol., 16, 1470–1486, 2010.

Dirnböck, T., Foldal, C., Djukic, I., Kobler, J., Haas, E., Kiese, R., and Kitzler, B.: Historic nitrogen deposition determines future climate change effects on nitrogen retention in temperate forests, Climatic Change, 144, 221–235, doi:10.1007/s10584-017-2024-y, https://doi.org/10.1007/s10584-017-2024-y, 2017.

Dise, N. B.: The European Nitrogen Assessment: Sources, Effects and Policy Perspectives, chap. 20, Cambridge University Press, 2011.

Donner, L. J., Wyman, B. L., Hemler, R. S., Horowitz, L. W., Ming, Y., Zhao, M., Golaz, J.-C., Ginoux, P., Lin, S.-J., Schwarzkopf, M. D., Austin, J., Alaka, G., Cooke, W. F., Delworth, T. L., Freidenreich, S. M., Gordon, C. T., Griffies, S. M., Held, I. M., Hurlin, W. J., Klein, S. A., Knutson, T. R., Langenhorst, A. R., Lee, H.-C., Lin, Y., Magi, B. I., Malyshev, S. L., Milly, P. C. D., Naik, V., Nath, M. J., Pincus, R., Ploshay, J. J., Ramaswamy, V., Seman, C. J., Shevliakova, E., Sirutis, J. J., Stern, W. F., Stouffer, R. J., Wilson, R. J., Winton, M., Wittenberg, A. T., and Zeng, F.: The Dynamical Core, Physical Parameterizations, and Basic Simulation Characteristics of the Atmospheric Component AM3 of the GFDL Global Coupled Model CM3, J. Clim., 24, 3484–3519, 2011.

Dore, A., Vieno, M., Tang, Y., Dragosits, U., Dosio, A., Weston, K., and Sutton, M.: Modelling the atmospheric transport and deposition of sulphur and nitrogen over the United Kingdom and assessment of the influence of SO2 emissions from international shipping, Atmospheric Environment, 41, 2355–2367, doi:10.1016/j.atmosenv.2006.11.013, https://doi.org/10.1016/j.atmosenv.2006.11.013, 2007.

Dore, A. J., Kryza, M., Hall, J. R., Hallsworth, S., Keller, V. J. D., Vieno, M., and Sutton, M. A.: The influence of model grid resolution on estimation of national scale nitrogen deposition and exceedance of critical loads, Biogeosciences, 9, 1597–1609, doi:10.5194/bg-9-1597-2012, https://doi.org/10.5194/bg-9-1597-2012, 2012.

Ellis, R. A., Jacob, D. J., Sulprizio, M. P., Zhang, L., Holmes, C. D., Schichtel, B. A., Blett, T., Porter, E., Pardo, L. H., and Lynch, J. A.: Present and future nitrogen deposition to national parks in the United States: critical load exceedances, Atmos. Chem. Phys., 13, 9083–9095, 2013.

Emmons, L. K., Walters, S., Hess, P. G., Lamarque, J.-F., Pfister, G. G., Fillmore, D., Granier, C., Guenther, A., Kinnison, D., Laepple, T., Orlando, J., Tie, X., Tyndall, G., Wiedinmyer, C., Baughcum, S. L., and Kloster, S.: Description and evaluation of the Model for Ozone and Related chemical Tracers, version 4 (MOZART-4), Geosci. Model Dev., 3, 43–67, 2010.

Erisman, J. W.: Evaluation of a surface resistance parametrization of sulphur dioxide, Atmos. Environ., 28, 2583–2594, 1994.

Erisman, J. W., Pul, A. V., and Wyers, P.: Parametrization of surface resistance for the quantification of atmospheric deposition of acidifying pollutants and ozone, Atmos. Environ., 28, 2595 – 2607, doi:http://dx.doi.org/10.1016/1352-2310(94)90433-2, http://www.sciencedirect.com/science/article/pii/1352231094904332, 1994.

Erisman, J. W., Hogenkamp, J. E. M., Putten, E. M. v., Uiterwijk, J. W., Kemkers, E., Wiese, C. J., and Mennen, M. G.: Long-term Continuous Measurements of SO_2 Dry Deposition over the Speulder Forest, Water. Air. Soil Pollut., 109, 237–262, doi:10.1023/A:1005097722854, http://link.springer.com/article/10.1023/A%3A1005097722854, 1999.

Erisman, J. W., Galloway, J. N., Seitzinger, S., Bleeker, A., Dise, N. B., Petrescu, A. M. R., Leach, A. M., and Vries, W. d.: Consequences of human modification of the global nitrogen cycle, Phil. Trans. R. Soc. B, 368, 20130 116, 2013.

Feliciano, M. S., Pio, C. A., and Vermeulen, A. T.: Evaluation of SO_2 dry deposition over short vegetation in Portugal, Atmos. Environ., 35, 3633–3643, 2001.

Finkelstein, P. L.: Deposition Velocities of SO_2 and O_3 over Agricultural and Forest Ecosystems, Water, Air and Soil Pollution: Focus, 1, 49–57, 2001.

Finkelstein, P. L., Ellestad, T. G., Clarke, J. F., Meyers, T. P., Schwede, D. B., Hebert, E. O., and Neal, J. A.: Ozone and sulfur dioxide dry deposition to forests: Observations and model evaluation, J. Geophys. Res. Atmos., 105, 15 365–15 377, 2000.

Flechard, C. R., Massad, R.-S., Loubet, B., Personne, E., Simpson, D., Bash, J. O., Cooter, E. J., Nemitz, E., and Sutton, M. A.: Advances in understanding, models and parameterizations of biosphere-atmosphere ammonia exchange, Biogeosciences, 10, 5183–5225, 2013.

Fleischer, K., Rebel, K. T., van der Molen, M. K., Erisman, J. W., Wassen, M. J., van Loon, E. E., Montagnani, L., Gough, C. M., Herbst, M., Janssens, I. A., Gianelle, D., and Dolman, A. J.: The contribution of nitrogen deposition to the photosynthetic capacity of forests, Global Biogeochem. Cycles, 27, 187–199, 2013.

Fleischer, K., Wårlind, D., van der Molen, M. K., Rebel, K. T., Arneth, A., Erisman, J. W., Wassen, M. J., Smith, B., Gough, C. M., Margolis, H. A., Cescatti, A., Montagnani, L., Arain, A., and Dolman, A. J.: Low historical nitrogen deposition effect on carbon sequestration in the boreal zone, J. Geophys. Res. Biogeosci., 120, 2015JG002 988, 2015.

Fowler, D., Flechard, C., Storeton-West, R. L., Sutton, M. A., Hargreaves, K. J., and Smith, R. I.: Long term measurements of SO2 dry deposition over vegetation and soil and comparisons with models, in: Studies in Environmental Science, edited by Erisman, G. J. H. a. J. W., vol. 64 of *Acid Rain Research: Do we have enough answers?Proceedings of a Specialty Conference*, pp. 9–19, Elsevier, 1995.

Fowler, D., Coyle, M., Skiba, U., Sutton, M. A., Cape, J. N., Reis, S., Sheppard, L. J., Jenkins, A., Grizzetti, B., Galloway, J. N., Vitousek, P., Leach, A., Bouwman, A. F., Butterbach-Bahl, K., Dentener, F., Stevenson, D., Amann, M., and Voss, M.: The global nitrogen cycle in the twenty-first century, Philos. Trans. R. Soc. London, Ser. B, 368, 2013.

Garland, J. A., Atkins, D. H. F., Readings, C. J., and Caughey, S. J.: Deposition of gaseous sulphur dioxide to the ground, Atmos. Environ., 8, 75–79, 1974.

Gerber, S., Hedin, L. O., Oppenheimer, M., Pacala, S. W., and Shevliakova, E.: Nitrogen cycling and feedbacks in a global dynamic land model, Global Biogeochem. Cycles, 24, GB1001, 2010.

Granat, L. and Richter, A.: Dry deposition to pine of sulphur dioxide and ozone at low concentration, Atmos. Environ., 29, 1677–1683, 1995.

Grizzetti, B.: The European Nitrogen Assessment: Sources, Effects and Policy Perspectives, chap. 17, Cambridge University Press, 2011.

Guenther, A., Karl, T., Harley, P., Wiedinmyer, C., Palmer, P. I., and Geron, C.: Estimates of global terrestrial isoprene emissions using MEGAN (Model of Emissions of Gases and Aerosols from Nature), Atmos. Chem. Phys., 6, 3181–3210, 2006.

Gundale, M. J., From, F., Bach, L. H., and Nordin, A.: Anthropogenic nitrogen deposition in boreal forests has a minor impact on the global carbon cycle, Glob. Chang. Biol., 20, 276–286, 2014.

Hertel, O.: The European Nitrogen Assessment: Sources, Effects and Policy Perspectives, chap. 14, Cambridge University Press, 2011.

Hicks, B. B.: Dry deposition to forests—On the use of data from clearings, Agric. For. Meteorol., 136, 214–221, doi:10.1016/j.agrformet.2004.06.013, http://www.sciencedirect.com/science/article/pii/S0168192305002066, 2006.

Hicks, B. B.: On Estimating Dry Deposition Rates in Complex Terrain, Journal of Applied Meteorology and Climatology, 47, 1651–1658, 2008.

Hicks, B. B., Baldocchi, D. D., Meyers, T. P., Hosker, R. P., and Matt, D. R.: A preliminary multiple resistance routine for deriving dry deposition velocities from measured quantities, Water, Air, & Soil Pollution, 36, 311–330, 1987.

Högberg, P.: What is the quantitative relation between nitrogen deposition and forest carbon sequestration?, Glob. Chang. Biol., 18, 1–2, 2012.

Huang, L., McDonald-Buller, E. C., McGaughey, G., Kimura, Y., and Allen, D. T.: The impact of drought on ozone dry deposition over eastern Texas, Atmos. Environ., 127, 176–186, doi:10.1016/j.atmosenv.2015.12.022, http://www.sciencedirect.com/science/article/pii/S1352231015305902, 2016.

Hurtt, G. C., Chini, L. P., Frolking, S., Betts, R. A., Feddema, J., Fischer, G., Fisk, J. P., Hibbard, K., Houghton, R. A., Janetos, A., Jones, C. D., Kindermann, G., Kinoshita, T., Goldewijk, K. K., Riahi, K., Shevliakova, E., Smith, S., Stehfest, E., Thomson, A., Thornton, P., Vuuren, D. P. v., and Wang, Y. P.: Harmonization of land-use scenarios for the period 1500–2100: 600 years of global gridded annual land-use transitions, wood harvest, and resulting secondary lands, Clim. Change, 109, 117–161, 2011.

Janssens, I. A., Dieleman, W., Luyssaert, S., Subke, J.-A., Reichstein, M., Ceulemans, R., Ciais, P., Dolman, A. J., Grace, J., Matteucci, G., Papale, D., Piao, S. L., Schulze, E.-D., Tang, J., and Law, B.: Reduction of forest soil respiration in response to nitrogen deposition, Nature Geosci, 3, 315–322, 2010.

Janssens-Maenhout, G., Crippa, M., Guizzardi, D., Dentener, F., Muntean, M., Pouliot, G., Keating, T., Zhang, Q., Kurokawa, J., Wankmüller, R., Denier van der Gon, H., Kuenen, J. J. P., Klimont, Z., Frost, G., Darras, S., Koffi, B., and Li, M.: HTAP_v2.2: a mosaic of regional and global emission grid maps for 2008 and 2010 to study hemispheric transport of air pollution, Atmos. Chem. Phys., 15, 11 411–11 432, doi:10.5194/acp-15-11411-2015, http://www.atmos-chem-phys.net/15/11411/2015/, 2015.

Jensen, N. O. and Hummelshøj, P.: Derivation of canopy resistance for water vapour fluxes over a spruce forest, using a new technique for the viscous sublayer resistance, Agric. For. Meteorol., 73, 339–352, 1995.

Jensen, N. O. and Hummelshøj, P.: Erratum, Agric. For. Meteorol., 85, 289, doi:10.1016/S0168-1923(97)00024-5, http://www.sciencedirect.com/science/article/pii/S0168192397000245, 1997.

Jickells, T., Baker, A. R., Cape, J. N., Cornell, S. E., and Nemitz, E.: The cycling of organic nitrogen through the atmosphere, Philos. Trans. R. Soc. London, Ser. B, 368, PMID: 23713115, 2013.

Johansson, O., Palmqvist, K., and Olofsson, J.: Nitrogen deposition drives lichen community changes through differential species responses, Glob. Chang. Biol., 18, 2626–2635, 2012.

Kalnay, E., Kanamitsu, M., Kistler, R., Collins, W., Deaven, D., Gandin, L., Iredell, M., Saha, S., White, G., Woollen, J., Zhu, Y., Leetmaa, A., Reynolds, R., Chelliah, M., Ebisuzaki, W., Higgins, W., Janowiak, J., Mo, K. C., Ropelewski, C., Wang, J., Jenne, R., and Joseph, D.: The NCEP/NCAR 40-Year Reanalysis Project, Bull. Am. Meteorol. Soc., 77, 437–471, 1996.

Lamarque, J.-F., Kyle, G., Meinshausen, M., Riahi, K., Smith, S., van Vuuren, D., Conley, A., and Vitt, F.: Global and regional evolution of short-lived radiatively-active gases and aerosols in the Representative Concentration Pathways, Clim. Change, 109, 191–212, 10.1007/s10584-011-0155-0, 2011.

Lamarque, J.-F., Dentener, F., McConnell, J., Ro, C.-U., Shaw, M., Vet, R., Bergmann, D., Cameron-Smith, P., Dalsoren, S., Doherty, R., Faluvegi, G., Ghan, S. J., Josse, B., Lee, Y. H., MacKenzie, I. A., Plummer, D., Shindell, D. T., Skeie, R. B., Stevenson, D. S., Strode, S., Zeng, G., Curran, M., Dahl-Jensen, D., Das, S., Fritzsche, D., and Nolan, M.: Multi-model mean nitrogen and sulfur deposition from the Atmospheric Chemistry and Climate Model Intercomparison Project (ACCMIP): evaluation of historical and projected future changes, Atmos. Chem. Phys., 13, 7997–8018, 2013.

Lepori, F. and Keck, F.: Effects of Atmospheric Nitrogen Deposition on Remote Freshwater Ecosystems, Ambio, 41, 235–246, doi:10.1007/s13280-012-0250-0, http://www.ncbi.nlm.nih.gov/pmc/articles/PMC3357855/, 2012.

Leuning, R.: A critical appraisal of a combined stomatal-photosynthesis model for C3 plants, Plant, Cell & Environment, 18, 339–355, 1995.

Levy, H., Horowitz, L. W., Schwarzkopf, M. D., Ming, Y., Golaz, J.-C., Naik, V., and Ramaswamy, V.: The roles of aerosol direct and indirect effects in past and future climate change, J. Geophys. Res. Atmos., 118, 4521–4532, 2013.

Li, Y., Schichtel, B. A., Walker, J. T., Schwede, D. B., Chen, X., Lehmann, C. M. B., Puchalski, M. A., Gay, D. A., and Collett, J. L.: Increasing importance of deposition of reduced nitrogen in the United States, Proc. Natl. Acad. Sci. U.S.A., p. 201525736, doi:10.1073/pnas.1525736113, http://www.pnas.org/content/early/2016/05/04/1525736113, 2016.

Loubet, B., Cellier, P., Milford, C., and Sutton, M. A.: A coupled dispersion and exchange model for short-range dry deposition of atmospheric ammonia, Quart. J. Roy. Meteor. Soc., 132, 1733–1763, 2006.

Magnani, F., Mencuccini, M., Borghetti, M., Berbigier, P., Berninger, F., Delzon, S., Grelle, A., Hari, P., Jarvis, P. G., Kolari, P., Kowalski, A. S., Lankreijer, H., Law, B. E., Lindroth, A., Loustau, D., Manca, G., Moncrieff, J. B., Rayment, M., Tedeschi, V., Valentini, R., and Grace, J.: The human footprint in the carbon cycle of temperate and boreal forests, Nature, 447, 849–851, 2007.

Malm, W. C., Rodriguez, M. A., Schichtel, B. A., Gebhart, K. A., Thompson, T. M., Barna, M. G., Benedict, K. B., Carrico, C. M., and Collett Jr., J. L.: A hybrid modeling approach for estimating reactive nitrogen deposition in Rocky Mountain National Park, Atmos. Environ., 126, 258–273, doi:10.1016/j.atmosenv.2015.11.060, http://www.sciencedirect.com/science/article/pii/S1352231015305677, 2016.

Malyshev, S., Shevliakova, E., Stouffer, R. J., and Pacala, S. W.: Contrasting Local versus Regional Effects of Land-Use-Change-Induced Heterogeneity on Historical Climate: Analysis with the GFDL Earth System Model, J. Clim., 28, 5448–5469, 2015.

Massad, R.-S., Nemitz, E., and Sutton, M. A.: Review and parameterisation of bi-directional ammonia exchange between vegetation and the atmosphere, Atmos. Chem. Phys., 10, 10 359–10 386, 2010.

Matsuda, K., Watanabe, I., Wingpud, V., Theramongkol, P., and Ohizumi, T.: Deposition velocity of O_3 and SO_2 in the dry and wet season above a tropical forest in northern Thailand, Atmos. Environ., 40, 7557–7564, 2006.

Matt, D. R., McMillen, R. T., Womack, J. D., and Hicks, B. B.: A comparison of estimated and measured SO2 deposition velocities, Water. Air. Soil Pollut., 36, 331–347, doi:10.1007/BF00229676, http://link.springer.com.ezproxy.princeton.edu/article/10.1007/BF00229676, 1987.

Meunier, C. L., Gundale, M. J., Sánchez, I. S., and Liess, A.: Impact of nitrogen deposition on forest and lake food webs in nitrogen-limited environments, Glob. Chang. Biol., 22, 164–179, doi:10.1111/gcb.12967, http://onlinelibrary.wiley.com/doi/10.1111/gcb.12967/abstract, 2016.

Meyers, T., Finkelstein, P., Clarke, J., Ellestad, T., and Sims, P.: A multilayer model for inferring dry deposition using standard meteorological measurements, Journal of Geophysical Research-Atmospheres, 103, 22 645–22 661, 1998.

Milly, P. C. D., Malyshev, S. L., Shevliakova, E., Dunne, K. A., Findell, K. L., Gleeson, T., Liang, Z., Phillipps, P., Stouffer, R. J., and Swenson, S.: An Enhanced Model of Land Water and Energy for Global Hydrologic and Earth-System Studies, J. Hydrometeorol., 15, 1739–1761, 2014.

Myles, L., Heuer, M. W., Meyers, T. P., and Hoyett, Z. J.: A comparison of observed and parameterized SO_2 dry deposition over a grassy clearing in Duke Forest, Atmos. Environ., 49, 212–218, 2012.

Naik, V., Horowitz, L. W., Fiore, A. M., Ginoux, P., Mao, J., Aghedo, A. M., and Levy, H.: Impact of preindustrial to present-day changes in short-lived pollutant emissions on atmospheric composition and climate forcing, J. Geophys. Res. Atmos., 118, 8086–8110, 2013.

Neirynck, J., Flechard, C. R., and Fowler, D.: Long-term (13 years) measurements of SO_2 fluxes over a forest and their control by surface chemistry, Agric. For. Meteorol., 151, 1768–1780, 2011.

Nemitz, E., Milford, C., and Sutton, M. A.: A two-layer canopy compensation point model for describing bi-directional biosphere-atmosphere exchange of ammonia, Quart. J. Roy. Meteor. Soc., 127, 815–833, 2001.

Nguyen, T. B., Crounse, J. D., Teng, A. P., Clair, J. M. S., Paulot, F., Wolfe, G. M., and Wennberg, P. O.: Rapid deposition of oxidized biogenic compounds to a temperate forest, Proc. Natl. Acad. Sci. U.S.A., 112, E392–E401, doi:10.1073/pnas.1418702112, http://www.pnas.org/content/112/5/E392, 2015.

Ochoa-Hueso, R., Allen, E. B., Branquinho, C., Cruz, C., Dias, T., Fen, M. E., Manrique, E., Pérez-Corona, M. E., Sheppard, L. J., and Stock, W. D.: Nitrogen deposition effects on Mediterranean-type ecosystems: An ecological assessment, Environ. Pollut., 159, 2265 – 2279, 2011.

Pardo, L. H., Fenn, M. E., Goodale, C. L., Geiser, L. H., Driscoll, C. T., Allen, E. B., Baron, J. S., Bobbink, R., Bowman, W. D., Clark, C. M., Emmett, B., Gilliam, F. S., Greaver, T. L., Hall, S. J., Lilleskov, E. A., Liu, L., Lynch, J. A., Nadelhoffer, K. J., Perakis, S. S., Robin-Abbott, M. J., Stoddard, J. L., Weathers, K. C., and Dennis, R. L.: Effects of nitrogen deposition and empirical nitrogen critical loads for ecoregions of the United States, Ecol. Appl., 21, 3049–3082, 2011.

Paulot, F., Crounse, J. D., Kjaergaard, H. G., Kroll, J. H., Seinfeld, J. H., and Wennberg, P. O.: Isoprene photooxidation: new insights into the production of acids and organic nitrates, Atmos. Chem. Phys., 9, 1479–1501, 2009.

Paulot, F., Jacob, D. J., and Henze, D. K.: Sources and Processes Contributing to Nitrogen Deposition: An Adjoint Model Analysis Applied to Biodiversity Hotspots Worldwide, Environ. Sci. Technol., 47, 3226–3233, 2013.

Paulot, F., Jacob, D. J., Pinder, R. W., Bash, J. O., Travis, K., and Henze, D. K.: Ammonia emissions in the United States, European Union, and China derived by high-resolution inversion of ammonium wet deposition data: Interpretation with a new agricultural emissions inventory (MASAGE_NH3), J. Geophys. Res. Atmos., 119, 4343–4364, 2014.

Paulot, F., Ginoux, P., Cooke, W. F., Donner, L. J., Fan, S., Lin, M.-Y., Mao, J., Naik, V., and Horowitz, L. W.: Sensitivity of nitrate aerosols to ammonia emissions and to nitrate chemistry: implications for present and future nitrate optical depth, Atmos. Chem. Phys., 16, 1459–1477, doi:10.5194/acp-16-1459-2016, http://www.atmos-chem-phys.net/16/1459/2016/, 2016.

Paulot, F., Fan, S., and Horowitz, L. W.: Contrasting seasonal responses of sulfate aerosols to declining SO_2 emissions in the Eastern U.S.: Implications for the efficacy of SO_2 emission controls, Geophys. Res. Lett., 44, 455–464, doi:10.1002/2016GL070695, http://dx.doi.org/10.1002/2016GL070695, 2016GL070695, 2017.

Phoenix, G. K., Emmett, B. A., Britton, A. J., Caporn, S. J. M., Dise, N. B., Helliwell, R., Jones, L., Leake, J. R., Leith, I. D., Sheppard, L. J., Sowerby, A., Pilkington, M. G., Rowe, E. C., Ashmore, M. R., and Power, S. A.: Impacts of atmospheric nitrogen deposition: responses of multiple plant and soil parameters across contrasting ecosystems in long-term field experiments, Glob. Chang. Biol., 18, 1197–1215, 2012.

Ponette-González, A. G., Weathers, K. C., and Curran, L. M.: Tropical land-cover change alters biogeochemical inputs to ecosystems in a Mexican montane landscape, Ecol. Appl., 20, 1820–1837, 2010.

Portmann, F. T., Siebert, S., and Döll, P.: MIRCA2000 — Global monthly irrigated and rainfed crop areas around the year 2000: A new high-resolution data set for agricultural and hydrological modeling, Global Biogeochem. Cycles, 24, GB1011, 2010.

Pregitzer, K. S., Burton, A. J., Zak, D. R., and Talhelm, A. F.: Simulated chronic nitrogen deposition increases carbon storage in Northern Temperate forests, Global Change Biol., 14, 142–153, 2008.

Ran, L., Pleim, J., Song, C., Band, L., Walker, J. T., and Binkowski, F. S.: A photosynthesis-based two-leaf canopy stomatal conductance model for meteorology and air quality modeling with WRF/CMAQ PX LSM, Journal of Geophysical Research: Atmospheres, 122, 1930–1952, doi:10.1002/2016jd025583, https://doi.org/10.1002/2016jd025583, 2017.

Reay, D. S., Dentener, F., Smith, P., Grace, J., and Feely, R. A.: Global nitrogen deposition and carbon sinks, Nat. Geosci., 1, 430–437, 2008.

Riahi, K., Rao, S., Krey, V., Cho, C., Chirkov, V., Fischer, G., Kindermann, G., Nakicenovic, N., and Rafaj, P.: RCP 8.5—A scenario of comparatively high greenhouse gas emissions, Clim. Chang., 109, 33–57, 2011.

Riddick, S., Ward, D., Hess, P., Mahowald, N., Massad, R., and Holland, E.: Estimate of changes in agricultural terrestrial nitrogen pathways and ammonia emissions from 1850 to present in the Community Earth System Model, Biogeosciences, 13, 3397–3426, doi:10.5194/bg-13-3397-2016, https://doi.org/10.5194/bg-13-3397-2016, 2016.

Rienecker, M. M., Suarez, M. J., Gelaro, R., Todling, R., Bacmeister, J., Liu, E., Bosilovich, M. G., Schubert, S. D., Takacs, L., Kim, G.-K., Bloom, S., Chen, J., Collins, D., Conaty, A., da Silva, A., Gu, W., Joiner, J., Koster, R. D., Lucchesi, R., Molod, A., Owens, T., Pawson, S., Pegion, P., Redder, C. R., Reichle, R., Robert-

son, F. R., Ruddick, A. G., Sienkiewicz, M., and Woollen, J.: MERRA: NASA's Modern-Era Retrospective Analysis for Research and Applications, J. Clim., 24, 3624–3648, 2011.

Sanderson, M. G., Collins, W. J., Hemming, D. L., and Betts, R. A.: Stomatal conductance changes due to increasing carbon dioxide levels: Projected impact on surface ozone levels, Tellus B, 59, doi:10.3402/tellusb.v59i3.17002, http://www.tellusb.net/index.php/tellusb/article/view/17002, 2007.

Schwede, D. B. and Lear, G. G.: A novel hybrid approach for estimating total deposition in the United States, Atmos. Environ., 92, 207–220, 2014.

Sheppard, L. J., Leith, I. D., Mizunuma, T., Neil Cape, J., Crossley, A., Leeson, S., Sutton, M. A., van Dijk, N., and Fowler, D.: Dry deposition of ammonia gas drives species change faster than wet deposition of ammonium ions: evidence from a long-term field manipulation, Glob. Chang. Biol., 17, 3589–3607, doi:10.1111/j.1365-2486.2011.02478.x, http://onlinelibrary.wiley.com/doi/10.1111/j.1365-2486.2011.02478.x/abstract, 2011.

Shevliakova, E., Pacala, S. W., Malyshev, S., Hurtt, G. C., Milly, P. C. D., Caspersen, J. P., Sentman, L. T., Fisk, J. P., Wirth, C., and Crevoisier, C.: Carbon cycling under 300 years of land use change: Importance of the secondary vegetation sink, Global Biogeochem. Cycles, 23, GB2022, 2009.

Simkin, S. M., Allen, E. B., Bowman, W. D., Clark, C. M., Belnap, J., Brooks, M. L., Cade, B. S., Collins, S. L., Geiser, L. H., Gilliam, F. S., Jovan, S. E., Pardo, L. H., Schulz, B. K., Stevens, C. J., Suding, K. N., Throop, H. L., and Waller, D. M.: Conditional vulnerability of plant diversity to atmospheric nitrogen deposition across the United States, Proc. Natl. Acad. Sci. U.S.A., 113, 4086–4091, doi:10.1073/pnas.1515241113, http://www.pnas.org/content/113/15/4086, 2016.

Simpson, D., Fagerli, H., Jonson, J., Tsyro, S., Wind, P., and Tuovinen, J.: The EMEP Unified Eulerian Model. Model Description. EMEP MSC-W Report 12003, The Norwegian Meteorological Institute, Oslo, Norway, 2003.

Singles, R., Sutton, M., and Weston, K.: A multi-layer model to describe the atmospheric transport and deposition of ammonia in Great Britain, Atmospheric Environment, 32, 393–399, doi:10.1016/s1352-2310(97)83467-x, https://doi.org/10.1016/s1352-2310(97)83467-x, 1998.

Smith, B., Wårlind, D., Arneth, A., Hickler, T., Leadley, P., Siltberg, J., and Zaehle, S.: Implications of incorporating N cycling and N limitations on primary production in an individual-based dynamic vegetation model, Biogeosciences, 11, 2027–2054, doi:10.5194/bg-11-2027-2014, https://doi.org/10.5194/bg-11-2027-2014, 2014.

Sorimachi, A., Sakamoto, K., Ishihara, H., Fukuyama, T., Utiyama, M., Liu, H., Wang, W., Tang, D., Dong, X., and Quan, H.: Measurements of sulfur dioxide and ozone dry deposition over short vegetation in northern China—a preliminary study, Atmos. Environ., 37, 3157–3166, 2003.

Stevens, C. J., Dise, N. B., Mountford, J. O., and Gowing, D. J.: Impact of Nitrogen Deposition on the Species Richness of Grasslands, Science, 303, 1876–1879, 2004.

Storkey, J., Macdonald, A. J., Poulton, P. R., Scott, T., Köhler, I. H., Schnyder, H., Goulding, K. W. T., and Crawley, M. J.: Grassland biodiversity bounces back from long-term nitrogen addition, Nature, 528, 401–404, doi:10.1038/nature16444, http://www.nature.com/nature/journal/v528/n7582/abs/nature16444.html, 2015.

Sutton, M., Nemitz, E., Erisman, J., Beier, C., Bahl, K. B., Cellier, P., de Vries, W., Cotrufo, F., Skiba, U., Marco, C. D., Jones, S., Laville, P., Soussana, J., Loubet, B., Twigg, M., Famulari, D., Whitehead, J., Gallagher, M.,

Neftel, A., Flechard, C., Herrmann, B., Calanca, P., Schjoerring, J., Daemmgen, U., Horvath, L., Tang, Y., Emmett, B., Tietema, A., Peñuelas, J., Kesik, M., Brueggemann, N., Pilegaard, K., Vesala, T., Campbell, C., Olesen, J., Dragosits, U., Theobald, M., Levy, P., Mobbs, D., Milne, R., Viovy, N., Vuichard, N., Smith, J., Smith, P., Bergamaschi, P., Fowler, D., and Reis, S.: Challenges in quantifying biosphere–atmosphere exchange of nitrogen species, Environmental Pollution, 150, 125–139, doi:10.1016/j.envpol.2007.04.014, https://doi.org/10.1016/j.envpol.2007.04.014, 2007.

Sutton, M. A., Simpson, D., Levy, P. E., Smith, R. I., Reis, S., Van Oijen, M., and De Vries, W.: Uncertainties in the relationship between atmospheric nitrogen deposition and forest carbon sequestration, Glob. Chang. Biol., 14, 2057–2063, 2008.

Sutton, M. A., Howard, C. M., Erisman, J. W., Billen, G., Bleeker, A., Grennfelt, P., Grinsven, H. v., and Grizzetti, B., eds.: The European Nitrogen Assessment: Sources, Effects and Policy Perspectives, Cambridge University Press, 2011.

Templer, P. H., Weathers, K. C., Lindsey, A., Lenoir, K., and Scott, L.: Atmospheric inputs and nitrogen saturation status in and adjacent to Class I wilderness areas of the northeastern US, Oecologia, 177, 5–15, 2014.

Townsend, A. R., Braswell, B. H., Holland, E. A., and Penner, J. E.: Spatial and Temporal Patterns in Terrestrial Carbon Storage Due to Deposition of Fossil Fuel Nitrogen, Ecol. Appl., 6, 806–814, 1996.

Tulloss, E. M. and Cadenasso, M. L.: Nitrogen deposition across scales: hotspots and gradients in a California savanna landscape, Ecosphere, 6, art167, doi:10.1890/es14-00440.1, https://doi.org/10.1890/es14-00440.1, 2015.

van Vuuren, D., Edmonds, J., Kainuma, M., Riahi, K., Thomson, A., Hibbard, K., Hurtt, G., Kram, T., Krey, V., Lamarque, J.-F., Masui, T., Meinshausen, M., Nakicenovic, N., Smith, S., and Rose, S.: The representative concentration pathways: an overview, Clim. Change, 109, 5–31, 2011.

Vieno, M., Dore, A. J., Wind, P., Marco, C. D., Nemitz, E., Phillips, G., Tarrasón, L., and Sutton, M. A.: Application of the EMEP Unified Model to the UK with a Horizontal Resolution of 5x 5 km2, in: Atmospheric Ammonia, pp. 367–372, Springer Netherlands, doi:10.1007/978-1-4020-9121-6_21, https://doi.org/10.1007/978-1-4020-9121-6_21, 2009.

Wang, Y., Jacob, D. J., and Logan, J. A.: Global simulation of tropospheric O_3-NO_x-hydrocarbon chemistry 1. Model formulation, J. Geophys. Res., 103, 10 713–10 726, 1998.

Wårlind, D., Smith, B., Hickler, T., and Arneth, A.: Nitrogen feedbacks increase future terrestrial ecosystem carbon uptake in an individual-based dynamic vegetation model, Biogeosciences, 11, 6131–6146, 2014.

Weathers, K. C., Lovett, G. M., Likens, G. E., and Lathrop, R.: The Effect of Landscape Features on Deposition to Hunter Mountain, Catskill Mountains, New York, Ecol. Appl., 10, 528–540, doi:10.2307/2641112, http://www.jstor.org/stable/2641112, 2000.

Weathers, K. C., Simkin, S. M., Lovett, G. M., and Lindberg, S. E.: Empirical Modeling of Atmospheric Deposition in Mountainous Landscapes, Ecol. Appl., 16, 1590–1607, 2006.

Wentworth, G. R., Murphy, J. G., Benedict, K. B., Bangs, E. J., and Collett Jr., J. L.: The role of dew as a night-time reservoir and morning source for atmospheric ammonia, Atmos. Chem. Phys., 16, 7435–7449, doi:10.5194/acp-16-7435-2016, http://www.atmos-chem-phys.net/16/7435/2016/, 2016.

Wesely, M. . L.: Parameterization of surface resistances to gaseous dry deposition in regional-scale numerical models, Atmos. Environ., 23, 1293–1304, 1989.

Williams, J. J., Chung, S. H., Johansen, A. M., Lamb, B. K., Vaughan, J. K., and Beutel, M.: Evaluation of atmospheric nitrogen deposition model performance in the context of U.S. critical load assessments, Atmospheric Environment, 150, 244–255, doi:10.1016/j.atmosenv.2016.11.051, https://doi.org/10.1016/j.atmosenv.2016.11.051, 2017.

Wolfe, A. P., Van Gorp, A. C., and Baron, J. S.: Recent ecological and biogeochemical changes in alpine lakes of Rocky Mountain National Park (Colorado, USA): a response to anthropogenic nitrogen deposition, Geobiology, 1, 153–168, 2003.

Wu, W. and Driscoll, C. T.: Impact of Climate Change on Three-Dimensional Dynamic Critical Load Functions, Environ. Sci. Technol., 44, 720–726, pMID: 20020745, 2010.

Wu, Z., Staebler, R., Vet, R., and Zhang, L.: Dry deposition of O_3 and SO_2 estimated from gradient measurements above a temperate mixed forest, Environ. Pollut., 210, 202–210, doi:10.1016/j.envpol.2015.11.052, http://www.sciencedirect.com/science/article/pii/S0269749115302128, 2016.

Wu, Z., Schwede, D. B., Vet, R., Walker, J. T., Shaw, M., Staebler, R., and Zhang, L.: Evaluation and intercomparison of five North American dry deposition algorithms at a mixed forest site, Journal of Advances in Modeling Earth Systems, doi:10.1029/2017ms001231, https://doi.org/10.1029/2017ms001231, 2018.

Zaehle, S., Friend, A. D., Friedlingstein, P., Dentener, F., Peylin, P., and Schulz, M.: Carbon and nitrogen cycle dynamics in the O-CN land surface model: 2. Role of the nitrogen cycle in the historical terrestrial carbon balance, Global Biogeochemical Cycles, 24, n/a–n/a, doi:10.1029/2009gb003522, https://doi.org/10.1029/2009gb003522, 2010.

Zhang, L., Gong, S., Padro, J., and Barrie, L.: A size-segregated particle dry deposition scheme for an atmospheric aerosol module, Atmos. Environ., 35, 549–560, 2001.

Zhang, L., Moran, M. D., Makar, P. A., Brook, J. R., and Sunling, G.: Modelling gaseous dry deposition in AURAMS: a unified regional air-quality modelling system, Atmos. Environ., 36, 537—560, 2002.

Zhang, L., Brook, J. R., and Vet, R.: A revised parameterization for gaseous dry deposition in air-quality models, Atmos. Chem. Phys., 3, 2067–2082, 2003.

Zhang, L., Jacob, D. J., Knipping, E. M., Kumar, N., Munger, J. W., Carouge, C. C., van Donkelaar, A., Wang, Y. X., and Chen, D.: Nitrogen deposition to the United States: distribution, sources, and processes, Atmos. Chem. Phys., 12, 4539–4554, 2012.

Zhu, L., Henze, D., Bash, J., Jeong, G.-R., Cady-Pereira, K., Shephard, M., Luo, M., Paulot, F., and Capps, S.: Global evaluation of ammonia bidirectional exchange and livestock diurnal variation schemes, Atmos. Chem. Phys., 15, 12 823–12 843, doi:10.5194/acp-15-12823-2015, http://www.atmos-chem-phys.net/15/12823/2015/, 2015.